NEW APPLICATION OF ACRIDINE ORANGE TO STUDY BIOPHYSICS OF EXOCYTOTIC PROCESSES IN CELL

by

DMYTRO SHUMILOV

Bachelor of Science, 2010
Kharkiv National University
Kharkov, Ukraine

Submitted to the Graduate Faculty of the
College of Science and Engineering
Texas Christian University
In partial fulfillment of the requirements
for the degree of

Master of Science

December 2013

ACKNOWLEDGMENTS

To my advisor, Dr. Gryczynski, gratitude is expressed for his support and participation. Thanks to Dr. Zerda for his corrections to the thesis. Thanks to Dr.Grygorczyk for his management of the cell imaging experiments.

TABLE OF CONTENTS

LIST OF FIGURES

INTRODUCTION

Within the last 30 years we have observed a significant growth of scientific interest in fluorescence applications to study molecular processes. Fluorescence has quickly become the technology of choice for molecular detection, biomedical diagnostics, and microscopy based imaging. What is more, advancements in chemistry have stimulated development of new probes allowing in-vitro and in-vivo labeling and enabling new biomedical applications. Today fluorescence is a leading technology for DNA detection (gene sequencing), protein studies, and cellular and tissue imaging. The incredible sensitivity of fluorescence based detection gave rise to single molecule detection (SMD) that allows observation and monitoring of molecular interactions on a fundamental (molecular) level. Quick progress in electronics and the development of various pulsed laser sources encouraged rapid development of time-resolved techniques that are applicable to microscopy advancing imaging techniques that include both cellular and tissue time-resolved measurements. Excellent resolution (fs and ms) made it possible to study dynamics of biomolecular processes naturally occurring in cell and tissue.

Herein I propose to utilize Acridine Orange (AO), a known fluorescence dye, for studying cellular processes. We have recently observed that fluorescence of AO strongly depends on its concentration. Spectra and fluorescence lifetimes change dramatically as the concentration of AO varies. At the same time it has been observed that AO tends to be accumulated in cellular vesicles. Vesicles are extruded into the extracellular space, breaking and releasing their contents into the solution causing dilution of AO. Exocytosis is a process by which cell directs chemical compounds out of its membrane. Concentration dependent behavior of AO could be a new, very sensitive way to follow cellular exocytotic processes. In this report I describe fluorescence properties of AO at various concentrations. Different methods applied to measuring absorption and fluorescence spectra, as well as time-resolved measurements, are described.

BACKGROUND

Luminescence Spectroscopy

Molecular luminescence spectroscopy studies measurements of light intensity produced by a sample that has been excited by light absorption or chemical reactions, but not by heating. The range of luminescence spectroscopy spreads from UV to visible and near IR light. Luminescent light is a result of emission of electro-magnetic (EM) radiation by an excited molecule, which returns from the excited state to the ground state. Luminescence can be divided into several categories according to the mechanism through which the molecule was excited. For example, in chemo luminescence the excited state of a molecule is produced by a chemical reaction; in photoluminescence it is achieved through absorption of a photon. Photoluminescence can be further divided into two groups, depending on the type of the excited state, fluorescence or phosphorescence.

Fluorescence is the emission of light from the excited singlet state. Since this type of transition is usually allowed within molecular orbitals, the emission rates of fluorescence are fast, on the order of $10^{-9}s^{-1}$. In contrast, phosphorescence is the emission of light from the triplet excited state, and this transition is typically forbidden. The emission rates are much slower, on the order of $10^{0}s^{-1}$ to $10^{3}s^{-1}$, therefore, phosphorescence lifetimes are usually much longer. The excitation of molecules by light occurs via interaction of molecular dipole transition moments with the electric field of the light wave and, to a much lesser extent, via interaction with the magnetic field of the light wave. [1]. First I will introduce absorbance as a measure of beam attenuation, and then I will describe interaction of the electromagnetic field of a light wave with a model two level atomic system.

Absorption of a Photon

Absorption of a photon is one of the most important phenomena in light and matter interaction.

The absorption measurement is the measurement of light extinction as a beam of light propagates through a sample. Due to light absorption the intensity of the beam decreases. Let's consider the following model. One can approximate the molecule as an opaque disk with the cross-sectional area σ, an effective area that is seen by the photon of frequency *v*. If the frequency of the photon is close to a resonance frequency, the cross-sectional area is maximal, otherwise the cross–section is 0. Considering a slab, *dz*, of the sample with total area *S*:

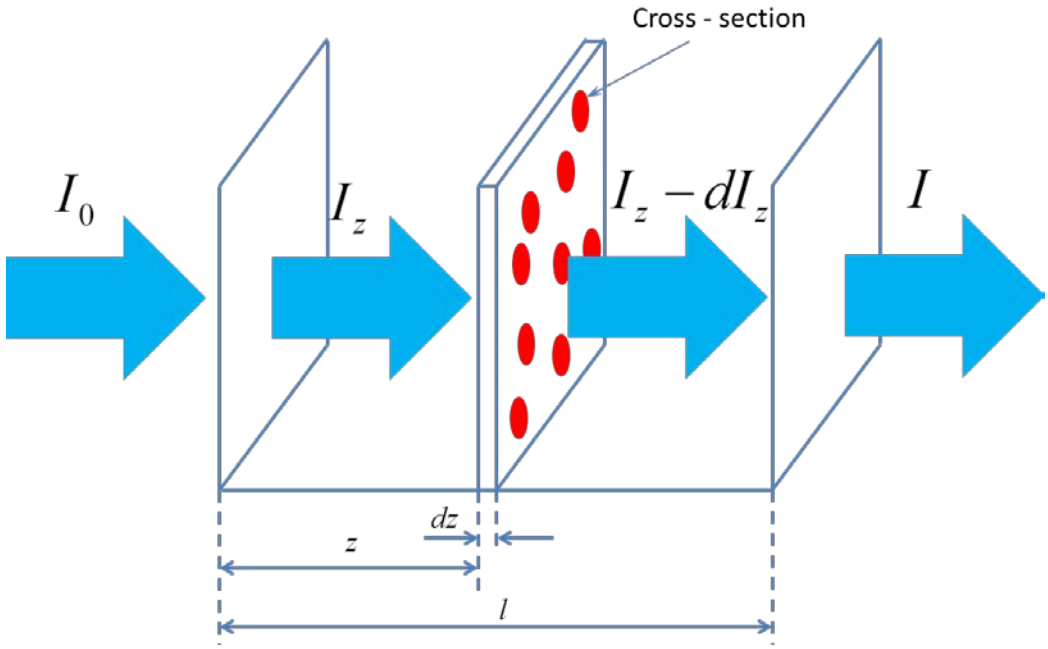

Figure 1. Absorption of light by molecules with defined cross-section

The total non-transparent area of the sample is $\sigma NSdz$, where N is number of molecules per cm^3. The fraction of absorbed photons is $\sigma NSdz/S$, so,

$$\frac{dI_z}{I_z} = -\sigma N dz \qquad (1)$$

I_z is the intensity of light entering the slab, and dI_z is intensity absorbed by the slab. The solution of equation (1) is obtained by integration of both sides:

$$\ln\left(\frac{I}{I_0}\right) = -\sigma N l \tag{2}$$

The ratio of the transmitted light intensity and the incident light intensity is called transmittance $T = I/I_0$. In absorption spectroscopy it is convenient to use molar concentration c and molar decadic extinction coefficient ε rather than cross – section, so with help of $\sigma = 1000\ln(10)\varepsilon/N_A$ and $\ln(I/I_0) = 2.303\log(I/I_0)$ equation (2) can be rewritten as:

$$\log\left(\frac{I}{I_0}\right) = -\varepsilon c l \qquad I = I_0 10^{-\varepsilon c l} \tag{3}$$

Absorbance is typically defined as $A = \varepsilon c l$ and it is a mathematical representation of the Beer – Lambert law which describes attenuation of the beam passing through the sample as a function of the molar decadic absorption coefficient, molar concentration of the absorbing specie and the thickness of the sample. Absorbance is measured in optical density units, O.D. [2]

Interaction of an Electromagnetic Wave with Matter in a Two-Level Atomic Model

Let's consider a set of N identical atoms with two bound-state energy levels E_0 and E_1. The difference between energies of the atomic levels can be expressed as:

$$\hbar\omega = E_0 - E_1 \tag{4}$$

where ω is the angular frequency of the photon that is required to bring an electron from the level E_0 to the level E_1. Atomic levels are singlets, the number of atoms in each state is N_1 and N_2 respectively and there are no other possible states, so $N_0+N_1=N$. The singlet state is formed by two electrons that have opposite spins. Electromagnetic radiation is not the only the way to bring an atom to the excited state, it is also possible to do it through thermal excitation. We can consider the average energy density of radiation of the system at frequency ω to consist of thermal density and externally applied electro-magnetic density of radiation (T and E subscripts respectively):

$$< W(\omega) >=< W_T(\omega) > + < W_E(\omega) > \tag{5}$$

Fluorescence measurements are conducted in the visible range where the energy contribution is much higher from electromagnetic radiation than from thermal excitation. It is possible to approximate the average density of the system as the density of an externally applied EM field: $<W(\omega)> = <W_E(\omega)>$. The probability of photon absorption and emission can be described as following. Consider an atom in an excited state E_1. There is a finite probability of spontaneous emission from this state, which will bring the photon with frequency ω to the ground state E_0. Probability per unit time for this process is A_{10} . This value is called the spontaneous emission rate. In the presence of radiation an atom can also be excited from the ground to the excited state. Probability of such a transition caused by absorption of the photon is B_{01}; we call it the absorption rate. Interaction of an excited atom with electromagnetic radiation is also possible. As a result another photon with the same frequency, phase and polarization is created. This process is called stimulated emission. Figure 2 schematically represents all three processes.

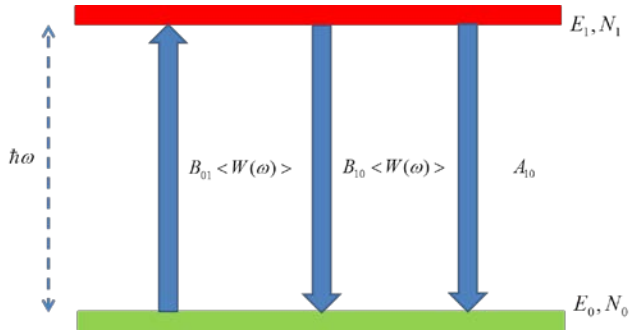

Figure 2. Interaction of electro-magnetic field with the set of two level atoms

A rate equation describes atoms populating the excited state and ground state:

$$\frac{dN_0}{dt} = -\frac{dN_1}{dt} = N_1 A_{10} - N_0 B_{01} < W(\omega) > + N_1 B_{10} < W(\omega) > \tag{6}$$

If the two level system is not degenerate, then $B_{01}=B_{10}=B$ and equation (6) becomes:

$$\frac{dN_0}{dt} = -\frac{dN_1}{dt} = N_1 A - N_0 B < W(\omega) > + N_1 B < W(\omega) > \tag{7}$$

Light sources used in fluorescence emission and lifetime measurements are unable to produce intensity that will make stimulated emission possible. Equation (7) can be simplified as

$$\frac{dN_0}{dt} = -\frac{dN_1}{dt} = N_1 A - N_0 B < W(\omega) > \tag{8}$$

Lifetime measurements require pulsed excitation. There is no illumination between exciting pulses, so $<W(\omega)>=0$ and the equation can be further simplified as:

$$\frac{dN_1}{dt} = -N_1 A \tag{9}$$

The spontaneous emission rate is connected with the natural lifetime of a fluorophore, which can be defined as the average time that an atom or a molecule spends in the excited state. However, this equation can be applied to a set of molecules too. Solution of equation (9) is:

$$N_1(t) = N_1(0)e^{-At} \tag{10}$$

I will present a detailed introduction to lifetime measurements in “Lifetimes measurements” section.[3]

Fluorescence Emission

The electronic structure of a fluorescent molecule has a more complex configuration than that of an atom and requires a more advanced model to describe its excitation and emission processes. Molecules which are excited as a result of the absorption of photons, tend to return to the ground state. Processes, which take place between absorption and emission of a photon, are shown on the Perrin-Jablonski diagram:

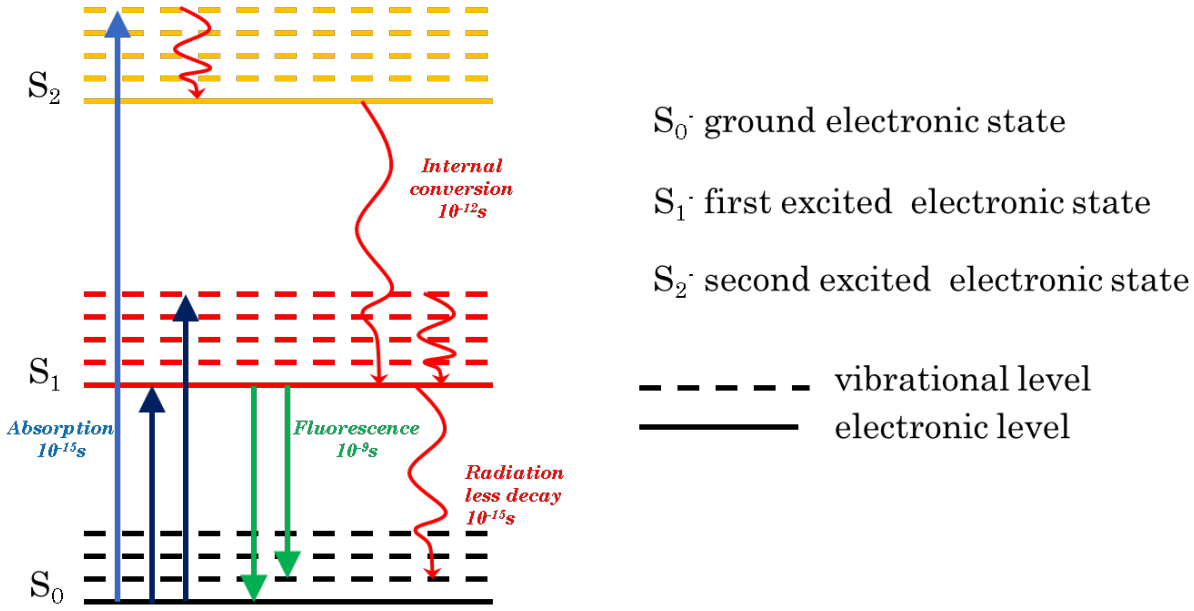

Figure 3. Perrin - Jablonski diagram

On this diagram the ground, first and second electronic states are denoted as, S_0, S_1 and S_2 respectively. The excited molecule can also exist in a number of vibrational states, which are transient and are shown on the diagram using dashed lines. Processes connected with photon absorption/emission are shown with vertical straight lines, radiation-less processes are depicted with curved lines. Internal conversion happens when a fluorescent molecule is excited to some vibrational levels of S_1 or S_2, then it quickly relaxes to the lowest vibrational level (approximately in $10^{-12}s$) of S_1 without the emission of a photon.

Emission typically occurs from the thermally equilibrated state, S_1, when a molecule returns in a single step to vibrational levels of the ground state S_0 or directly to S_0. Fluorescence

emission spectra do not depend on the excitation wavelength; this is Kasha's rule. Such behavior is explained by the following: molecules, which are excited with excess energy, rapidly relax to S_1 due to internal conversion and then might emit light when returning to the ground state. Some molecules might emit directly from S_2, but in biological systems such molecules are rare. Emission occurs at longer wavelengths than absorption, the phenomenon called Stoke's shift (Figure 4). [4,5]

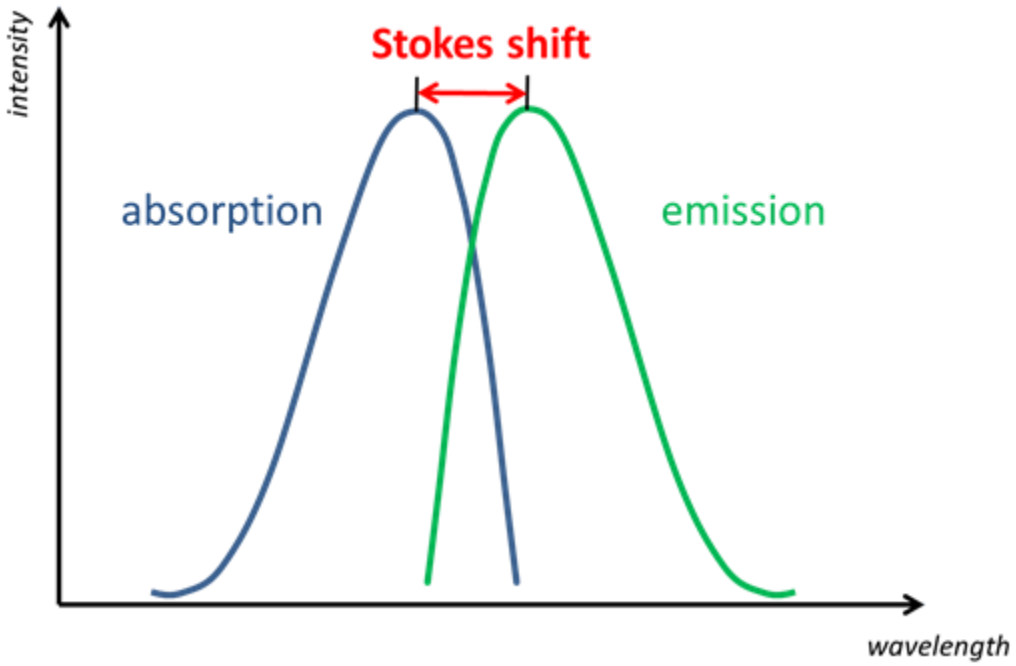

Figure 4. Stoke's shift

Absorption Spectroscopy

Absorption spectroscopy measures intensity of light that has passed through the sample and then compares it to the intensity of incident light, determining how much light was absorbed by the sample (Figure 5). Typical absorption measurements are performed in a 10 x 10mm cuvette. Most spectrometers have a dynamic range for absorption measurement from 0 to 3 O.D. Optical densities of 3 corresponds to light attenuation of 10^3. The O.D. unit represents the logarithmic ratio of transmitted light intensity to the incident light intensity; also it can also be expressed as a negative logarithm of transmittance T:

$$A = -\log \frac{I_1}{I_0} = -\log T \tag{11}$$

High quality absorption measurements on most instruments are limited to 2 O.D. because at very high sample density the intensity difference between the sample and no-sample (reference) measurements is too high and the nonlinear response of the detector may perturb the measurement.

The schematic of a typical spectrophotometer is presented in Figure 5. Absorbance of the light is measured for each wavelength and is plotted as a function of the wavelength.

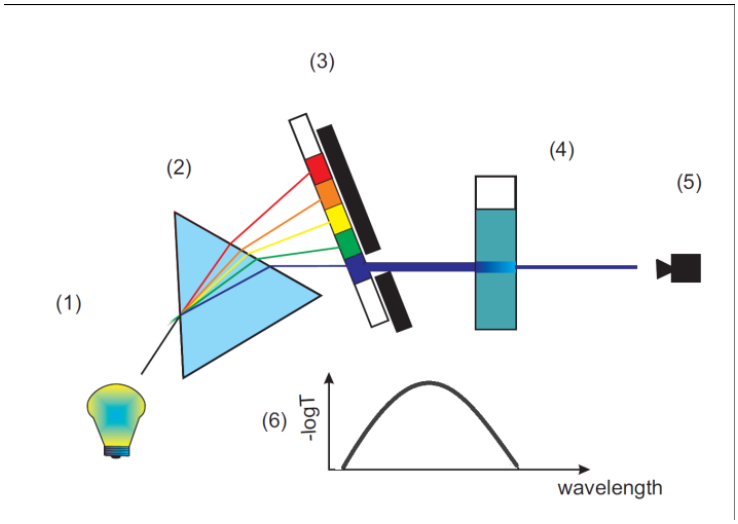

1	white light source (all wavelengths)
2	separate into wavelengths
3	select proper color with a slit
4	light transmission through the sample
5	transmitted light intensity is measured
6	plot –log T as a function of wavelength

Figure 5. Absorption spectrometer scheme

Fluorescence Spectroscopy

A typical spectrofluorometer has the following geometry: a detector is placed at 90° to an excitation source (Figure 6). The excitation source can be a lamp or a laser. Lamps with a monochromator can provide many desired wavelengths. The quality of monochromatic light depends on the quality of the monochromator. Instead of a lamp with a monochromator one can also use a laser as the source of monochromatic light. An additional advantage of using lasers is their high intensity, which can be useful for low concentration samples.

The detection of emitted light also requires a monochromator, which scans the wavelengths. Measurements typically start 5 – 20 nm after the excitation wavelength to prevent leakage of scattered excitation light. To eliminate any polarization effect in the measurements, an excitation polarizer is placed at 0° and emission at 54.7°, the so called magic angle. The magic angle is obtained from the Malus law. Malus law relates intensity of light that passes through the polarizer to the intensity of transmitted light: $I = I_0 cos^2 \theta$, where I is transmitted intensity, I_0 is initial intensity and θ is the angle between light's initial polarization and the axis of the polarizer. Positioning the detector at 90° to the excitation source minimizes the direct penetration or reflection of excitation light into the monochromator. [6,7]

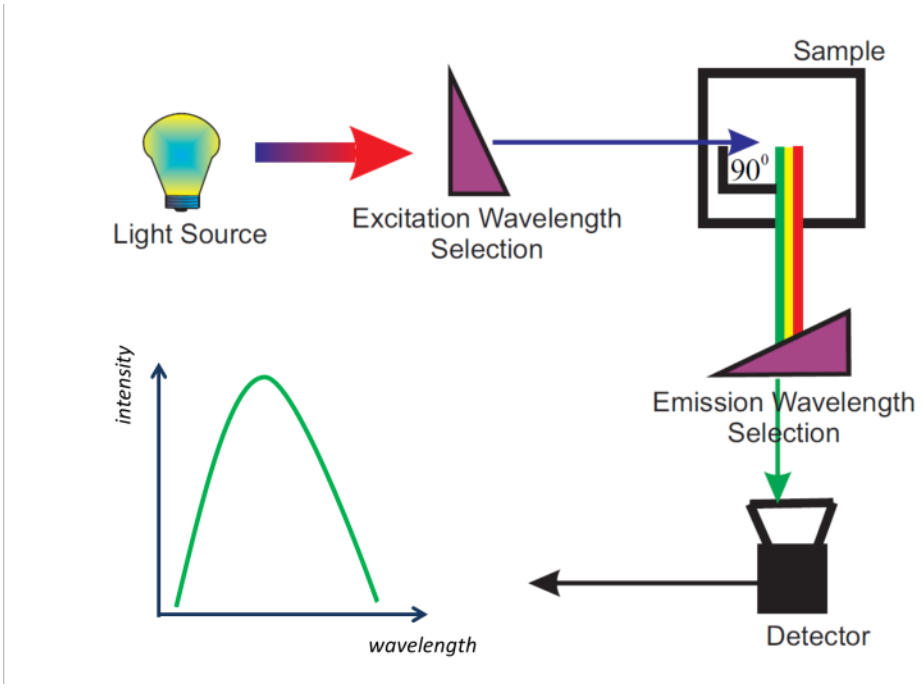

Figure 6. Spectrofluorometer scheme

Fluorescence Quantum Yield

Fluorescence quantum yield (Q) quantitatively describes the ratio of the number of photons that were emitted to the number of photons that were absorbed.

$$Q = \frac{number\ of\ molecules\ that\ emitted\ a\ photon}{total\ number\ of\ excited\ molecules} \tag{12}$$

It is necessary to understand that equal numbers of emitted and absorbed photons (100% quantum yield) do not imply equal amounts of absorbed and emitted energies. Emitted photons have longer wavelengths, that is, lower energies. In the simplest case, the emission process is described by the radiative rate, Γ, and the nonradiative decay rate, k_{nr} that represent nonradiative processes leading to excited state deactivation (cumulative for all nonradiative processes mentioned previously). In terms of described rates quantum yield Q can be defined as:

$$Q = \frac{\Gamma}{\Gamma + k_{nr}} \tag{13}$$

Quantum yield approaches 100% when $\Gamma >> k_{nr}$.[7]

Fluorescence Lifetime

An important characteristic of fluorescence is a significant finite time between the excitation process and the emission process called fluorescence lifetime. As mentioned before, the rates for deactivation of the excited singlet state are providing lifetimes that are typically on the order of nanoseconds. Importantly deactivation of the excited state is a statistical process and fluorescence lifetime represents the average time a molecule spends in the excited state. Fluorescence lifetime contains information about the molecule (a fluorophore) and is independent from many factors such as excitation wavelength, excitation power, and to a large extent, molecular concentration. Because of that it might provide important information about the molecular system. For example, multi-exponential decay can supply information about the intermolecular interaction of a fluorophore with solvent or various complex formations. Macromolecules often can exist in different conformations, and multi- exponential decays of a fluorophore can give information about the number of conformational states. The fluorescence lifetime can be expressed through deactivation rates as:

$$\tau = \frac{1}{\Gamma + k_{nr}} \tag{14}$$

The lifetime τ describes an average time that molecules spend in the excited state. If we recall the equation for spontaneous emission (9), replace radiative rate A with Γ and consider nonradiative rates, assuming that initially $N_0=N(t_0)$ molecules were excited by an infinitely short pulse of light, then the number of molecules in the excited state can be described as a function of time by the following rate equation:

$$\frac{dN(t)}{dt} = -(\Gamma + k_{nr})N(t) \tag{15}$$

The solution of equation (9) describes the evolution (decay) of excited molecule populations in the absence of illumination and represents fluorescence intensity decay, which for a single exponential is:

$$N(t) = N_0 e^{-t(\Gamma + k_{nr})} = N_0 e^{-\frac{t}{\tau}} \tag{16}$$

Intensity decay is a statistical process, and molecules in an excited state can be found after times longer that the fluorescence lifetime, τ. The decay can be also multi-exponential in cases of complex structure of a molecule or simply because different types of molecules are present in the mixture.

$$N(t) = \sum_i N_{0i} e^{-t(\Gamma + k_{nr})_i} = \sum_i N_{0i} e^{-\frac{t}{\tau_i}} \tag{17}$$

Due to the high sensitivity of fluorescence lifetimes to the environment surrounding a fluorophore, fluorescence lifetime measurements have many practical applications, especially in biology. [7,9]

Lifetime Measurements

Lifetime measurements require more advanced instrumentation than emission spectra measurements, as well as more complex software for collecting and analyzing data. The most popular types of fluorescence lifetime measurements are time domain, frequency domain, and streak camera measurements [8]. Herein I will only describe time domain measurements. [8,9]

Ideally, a sample is excited by an infinitely sharp pulse, which is considered to be a δ – function. As a result, an initial excited state population is created (Figure 7). The number of excited molecules at subsequent times can be described by the exponential model described by equation (15).

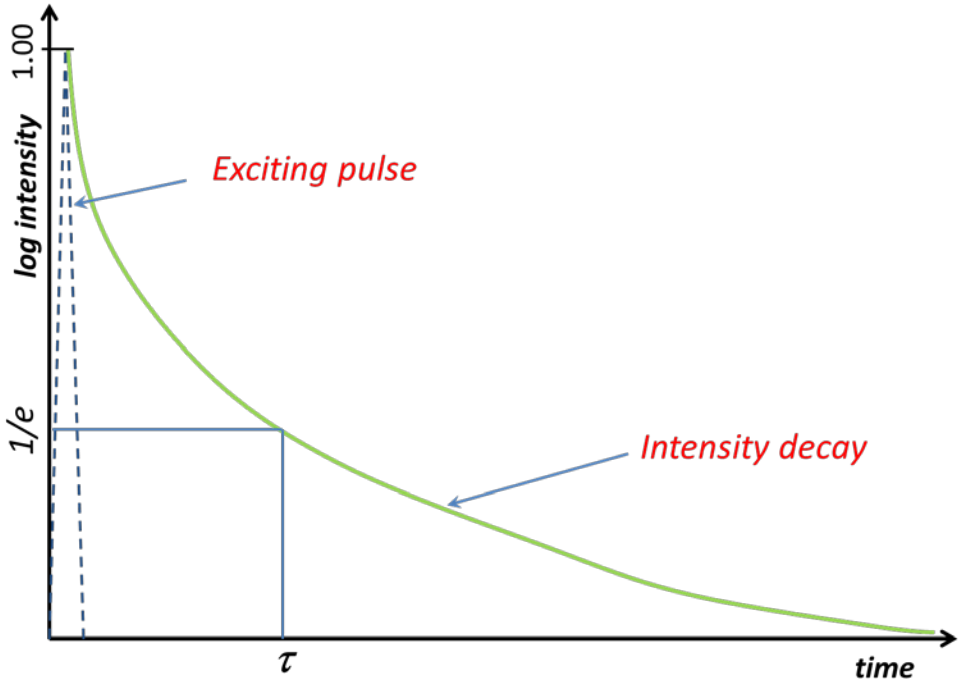

Figure 7. Simulation of fluorescence intensity decay

Analysis of intensity decay data is a complex procedure that involves deconvolution of the excitation pulse, instrument response and experimental model to the assumed decay.

Fluorescence lifetime measurements are typically performed in the same geometrical configuration as steady state measurements. A light beam is directed onto the sample at 90° to the detector to prevent excitation light leaking into it. An emission monochromator or a narrow bandpass filter is used for selection of the observation wavelength. An excitation monochromator

or filters can also be used if the excitation source is a flashlamp or a multiwavelength pulsed light source, for instance, the super-continuum laser. Our laboratory is equipped with PicoQuant FT300, a fluorescence spectrometer, based on Time Correlated Single Photon Counting (TCSPC) technique. [8]

Time Correlated Single Photon Counting

Most modern time domain system measurements utilize the time-correlated single photon counting technique. I will outline the basic principles of TCSPC and describe various instrumentations used.

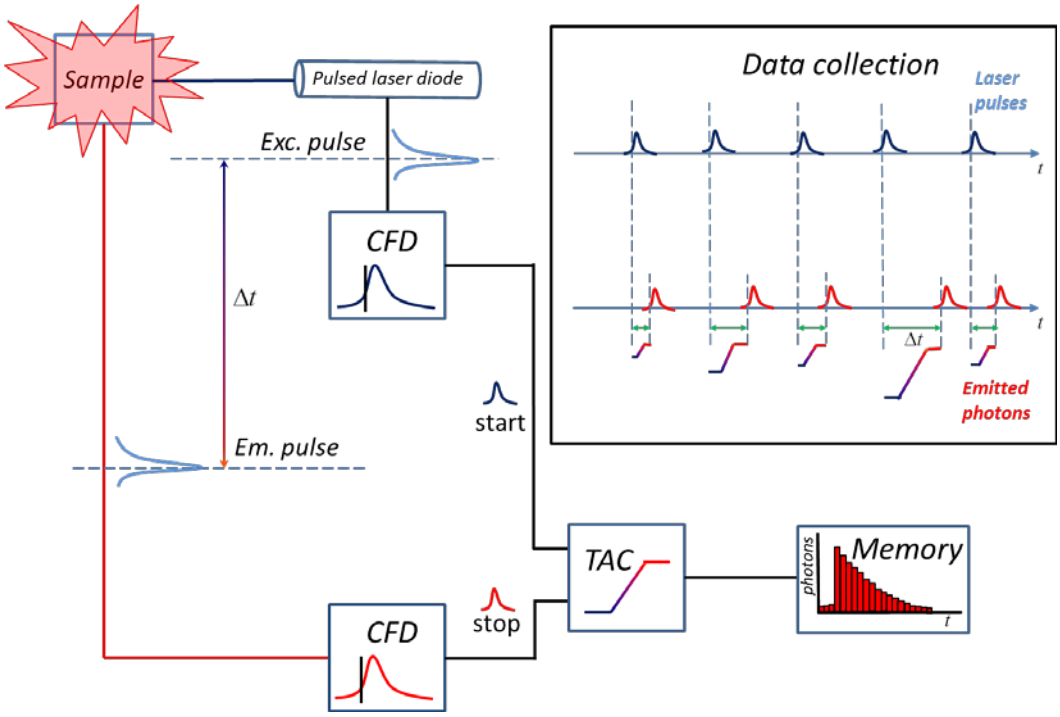

Figure 8. Time Correlated Single Photon Counting instrumental scheme

A sample is excited with a pulsed light source with constant repetition rate. The repetition rate is the frequency of the pulsing laser. The detection process is started with an excitation pulse that excites the sample and activates the electronics (Figure 8). The CFD, constant fraction discriminator, determines the time of the laser pulse arrival very precisely [8]. Start and stop pulses can have amplitude jitter that may cause time jitter in the order of pulse's rise time. CFD's electronics are designed to eliminate these effects and determine accurate arrival time of the pulse. CFD also eliminates all possible background pulses produced in the detector, leaving only the signal. Then the TAC, time to amplitude converter, generates a voltage ramp that is stopped by another signal from the CFD, which is generated after the photon has arrived.

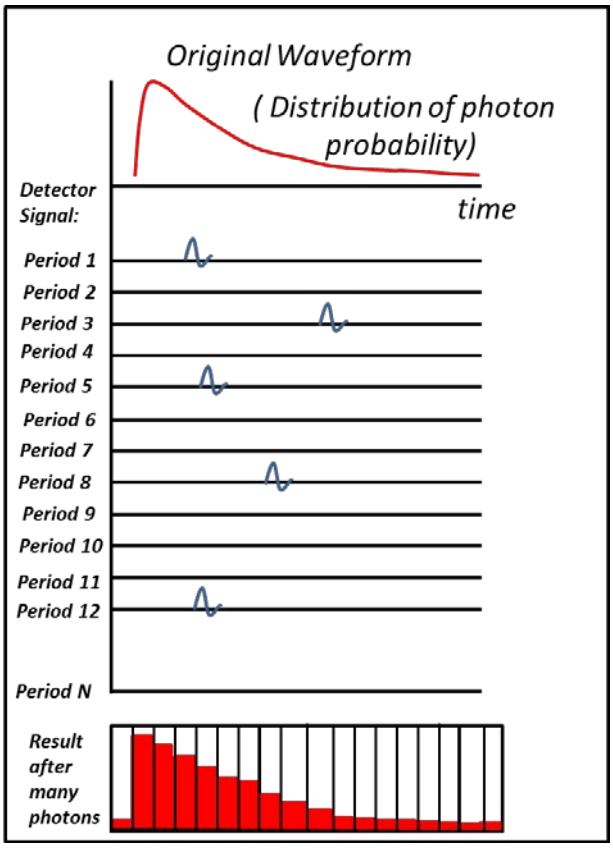

Figure 9. Distribution of the detected photons across the time channels

As a result, the TAC contains voltage that is proportional to the time between the initial and the detected pulse. The transformed TAC signal is stored in the address of the memory corresponding to the appropriate delay time. If no photon arrives, the cycle starts again with a new laser pulse. The time distribution of photon probability is displayed in the top part of Figure 9. Intensity of light is considered to be low enough so that the probability of detecting two or more photons in one signal period is negligibly small. The signal period is the time between exciting pulses. The detection rate usually varies from 0.1 to 0.01 photons per signal period. Higher detection rates cause shortening of the lifetimes since only the very first channel detects photons, and measurements will not provide the correct lifetime. Time scale is divided by the number of detector channels. When the measurement is completed, distribution of photons across the detector channels (bottom of Figure 9) is generated. [8,9,10].

TCSPC Data Analysis (Fitting)

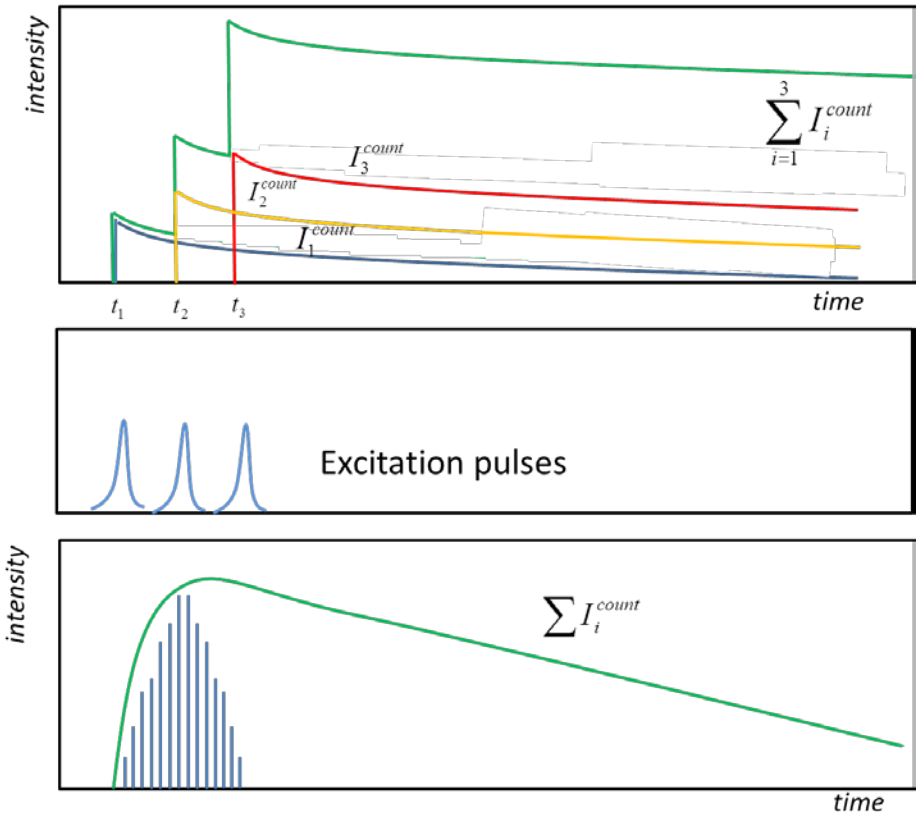

Figure 10. Convolution of lamp function response and decay

When the excitation pulse cannot be approximated by a delta function, the effect of signal broadening by the finite width of the pulse must be considered. Measured intensity decay is convoluted with the excitation source function, a 'lamp function'. It is so called so because it is impossible to measure the impulse response function directly. Most instruments have a response function approximately 0.05–2 ns wide. The excitation pulse can be interpreted as a series of δ-functions with different intensities (Figure 10). Each particular δ-function of the pulse excites an impulse response from the sample proportionally to its height. The intensity is proportional to the number of molecules in the excited state. Mathematically it can be expressed as:

$$I^{count}(t) = \int_0^{t_i} L(t) I(t_i - t) dt \tag{18}$$

where $L(t)$ is the lamp function. The term $(t_i–t)$ appears here because impulse response is started at $t=t_i$ and there are no molecules in the excited states before the excitation $(t_i < t)$. For convenience, equation (18) can be rewritten as [9, 10]:

$$I^{count}(t_i) = \int_0^{t_i} L(t_i - t) I_0 e^{-t/\tau} dt \tag{19}$$

The obtained signal is a convolution of the lamp function and the real intensity decay. Real intensity decay $I_0e^{-t/\tau}$ is obtained after deconvolution. Intensity decay represents the distribution of the photons' arrival time. An exponential function is typically used to fit obtained data. The total goodness of fit (χ^2) is expressed as a sum of corresponding variables:

$$\chi^2 = \sum_{i=1}^{n} \left[\frac{N^{ob}(t_i) - N^{cal}(t_i)}{\eta_i} \right]^2 \tag{20}$$

Where N^{ob} is the number of counts in a time channel, N^{cal} is appropriate value of the fitting function. Standard deviation (η_i) is considered to be proportional to the square root of the number of counts in a channel:

$$\chi^2 = \sum_{i=1}^{n} \left[\frac{N^{ob}(t_i) - N^{cal}(t_i)}{\sqrt{N^{ob}}(t_i)} \right]^2 \tag{21}$$

χ^2 depends on the number of data points, so it is not the best way to judge goodness of the fit. Most fitting software use reduced chi squared (χ_R^2), which represents standard weighted least squares for the set of experimental data points and is represented by:

$$\chi_R^2 = \frac{1}{n} \sum_{i=1}^{m} \chi_i^2 = \frac{1}{n} \sum_{i=1}^{m} \left[\frac{N^{ob}(t_i) - N^{cal}(t_i)}{\sqrt{N^{ob}}(t_i)} \right]^2 \tag{22}$$

where n is the number of data points minus the number of fitting parameters, and m is the number of data points. Usually chi squared number around 1 represents a good fit, and the lifetimes obtained from particular experiment are considered to be reliable. [11,12]

INSTRUMENTATION

FluoTime 300 Description

FT 300 is a fluorescent spectrometer with fluorescent lifetime measurements and emission spectra measurements capability. The system layout (adopted from PicoQuant FT 300 manual) is depicted on the Figure 11:

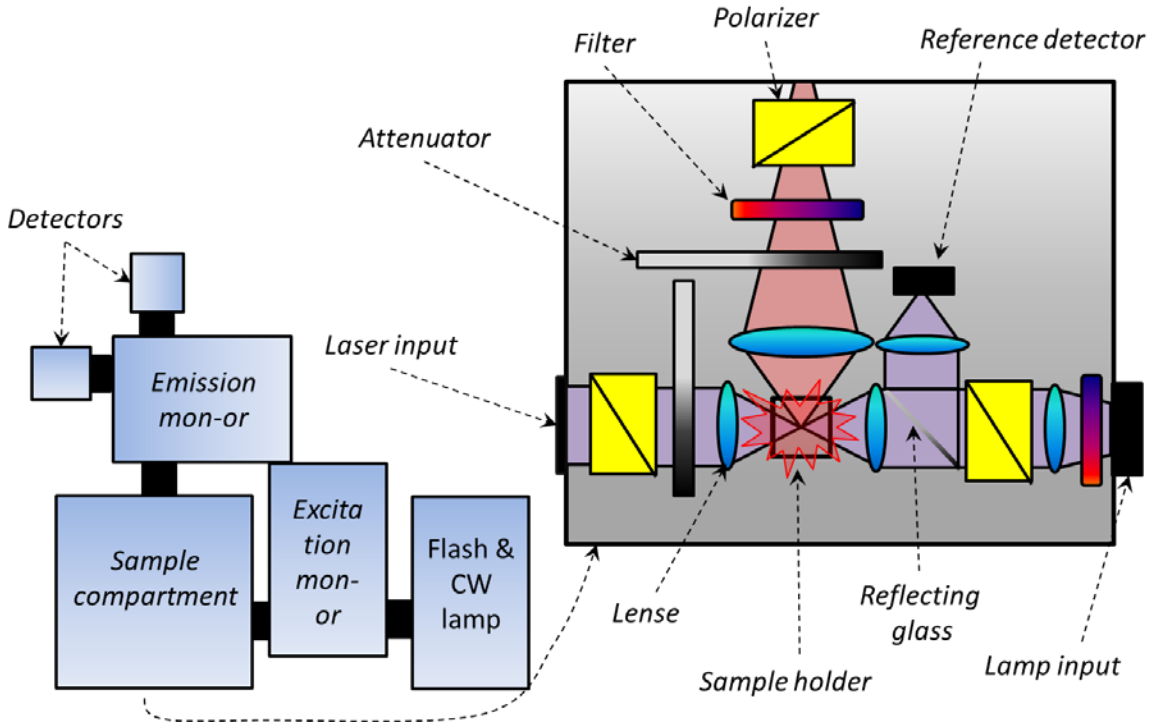

Figure 11. FluoTime 300 instrument layout

The FluoTime 300 is designed to measure maximum emission light throughput and has very high sensitivity. This is achieved by utilizing the single photon counting data acquisition methods and careful design and selection of all optical components [13]. It uses the same technique for steady state measurements as for TCSPC, an important feature that makes this particular instrument different from analog spectrometers. Regular spectrometers performing this type of measurements use voltage produced by a photomultiplier tube (PMT) after it detects a photon. The FT 300 uses photon counts, not voltage to determine fluorescence intensity. This makes it possible to collect and discern spectra from femtomolar concentrations of a fluorophore, mainly

because of very low signal to noise ratio. Another unique feature of this instrument is the possibility of collecting emission spectra, excitation spectra, and performing time-resolved measurements on exactly the same spot, without moving the sample. This increases the precision of measurements, especially for solid samples, which can often be non-uniform. The FT300 can also excite a sample with two light sources: a lamp and a laser. The FT300 can operate as a spectrometer and a time-resolved measurement system and can combine these two types of measurements. Its high sensitivity in steady state measurements makes it a powerful fluorescence spectroscopy tool. The instrument is totally automated and is controlled by its software. The fitting routine communicates with the main software, but it is also possible to use it on separate computers for advanced data analysis.

RESEARCH MOTIVATION

Acridine Orange (AO)

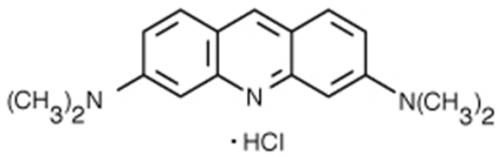

Figure 12. Molecular structure of Acridine Orange

Acridine orange is a fluorescent dye that has been known and used for over 50 years [14] (Figure 12). Its molar mass is 265.35 g/mol, and it is soluble in water, in concentration 28 g/L [14]. Acridine orange is also used as a DNA intercalator [15] and has been used for DNA studies for over 20 years. Intercalation is the reversible inclusion of a molecule between two other molecules. Intercalation can be monitored by fluorescence emission. At low concentrations, (starting at 0.05 g/L) AO spectra are similar to those of fluorescein, an organic fluorescence dye. It has an absorption maximum around 494 nm and an emission wavelength of 525 nm. When AO binds to DNA or RNA, the emission properties change significantly and emission peak may shift up to 640 nm.

It has been observed that absorption spectra, emission spectra, and fluorescence lifetimes of AO strongly depend on concentration. The change of these properties is due to aggregates formation at high concentrations. Highly concentrated AO solution preferentially contains aggregates, but dilution causes production of monomers. Intermediate concentrations contain a mixture of both. We expect aggregates to be dimers. Dimer formation can be explained by p stacking of benzene rings of two AO monomers, p stacking is attractive interaction of the benzene rings. Also it has been observed that AO exclusively accumulates in cellular vesicles [16] that have low pH (~5.5).

Mucus Secretion as an Example of an Exocytotic Process

Mucus secretion is the first line of defence against the barrage of irritants inhaled into human lungs during breathing.[17,18] Mucus forms a thin film of viscoelastic gel on the surface of the airways that protects the epithelial cells by entrapping foreign debris, bacteria, and viruses, and clearing them from the airway by ciliary movement, a process termed mucociliary clearance. In case of a disease such as cystic fibrosis (CF) [20], asthma, or chronic obstructive pulmonary disease (COPD) [19], excessive production of mucus (hypersecretion), as well as changes in its viscoelastic properties result in accumulation of thick, sticky mucus in the lungs, effectively impairing the mucociliary clearance process. This leads to difficulty in breathing, morbidity, and in severe cases, mortality [29]. 1% to 2% of mucus gel comprises mucin glycoproteins that are secreted by specialized cells. They are polyanionic macromolecules that are stored in cytoplasmic granules in a highly condensed state. Upon stimulation they are rapidly secreted, in hundreds of milliseconds, by an exocytotic process and undergo enormous several-hundred-fold swelling/expansion. Despite its importance in airway physiology, our understanding of cellular mechanisms of mucus release is rudimentary. For example, we do not know the sequence of intracellular events leading to mucus granule secretion, as well as the exact processes regulating post-exocytotic mucin expansion. Current video and microscopy technology for studying the physiology of the mucus secretion process lags well behind its biochemical/genetic characterization. This is mostly due to the fact that the secretion process is very rapid (unfolds in tens of milliseconds) and to the lack of well characterized fluorescent mucin labels. [21,22]

EXPERIMENTS

The goal of this study is to characterize fluorescent properties of AO as a function of its concentration. To explore fluorescent properties we measure the quantum yield and extinction coefficient. Fluorescence spectra and fluorescence lifetime measurements reveal significant changes due to aggregation, and these properties can be useful for determination of mucus expansion since fluorescence lifetimes change as concentration of AO decreases.

Preliminary Results of Experiments Measuring Lifetimes

Herein I present the set of steady-state and time-resolved experiments with well-known dyes frequently used as standards. The purpose of these experiments is to demonstrate the possibility of detecting single and multiple lifetime components and establishing precision of these measurements, used later for AO study. Three dyes with known lifetimes were selected: Erythrosine B (lifetime ~ 0.6 ns), Rhodamine B (lifetime ~ 2.8 ns), DAOTA (lifetime ~ 19 ns). The dyes were dissolved in ethanol and their absorption spectra were measured in a cuvette. For the concentrations used the absorption at 487 nm for all three dyes is identical so it was selected as the excitation wavelength (Figure 13).

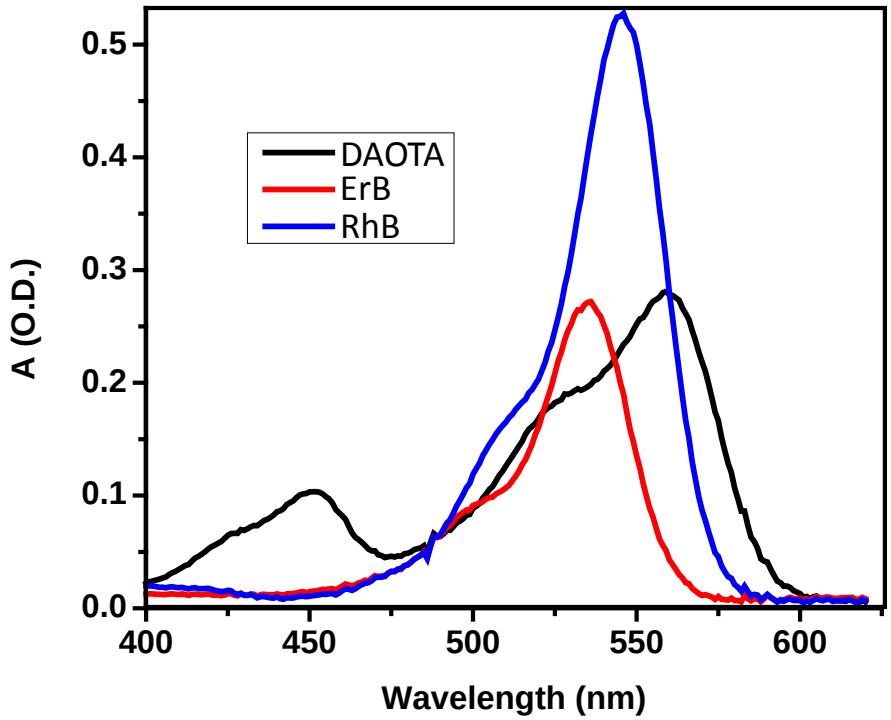

Figure 13. Absorption spectra of DAOTA, ErB and RhB

Emission spectra of the dyes and their mixtures in equal proportions were also measured and normalized (Figure 14):

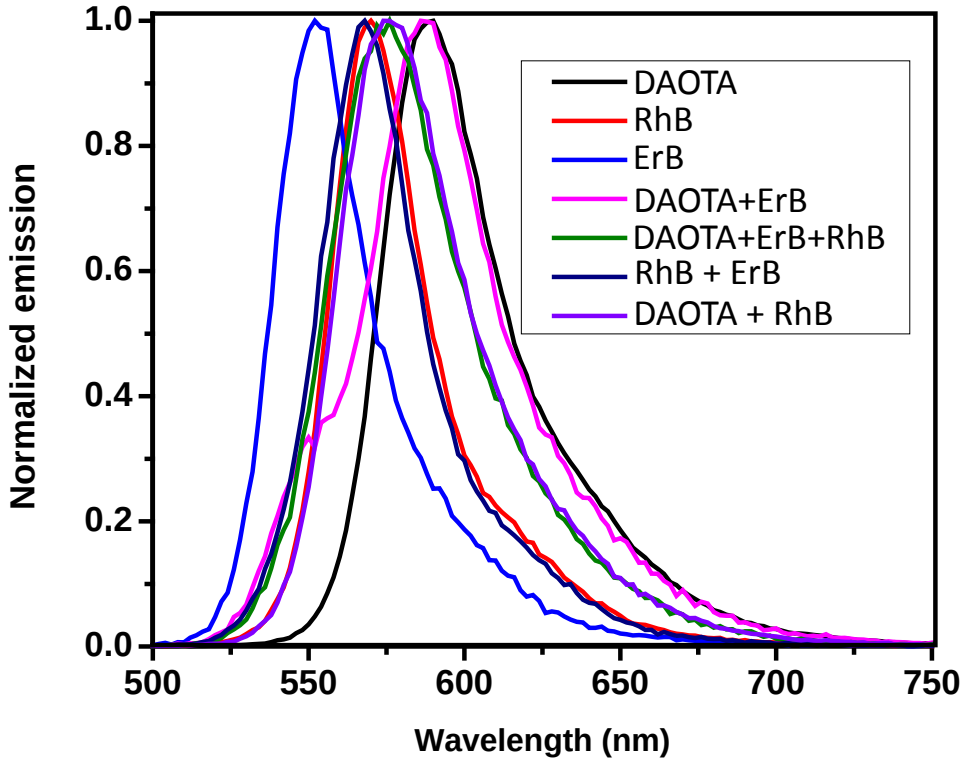

Figure 14. Normalized emission spectra of DAOTA, ErB, RhB and their mixtures

Looking at normalized emission spectra, one can to see that RhB has highest Q because its emission (540 nm) dominates in mixtures, regardless of the fact that absorption is equal for all three dyes, and mixtures are prepared with equal amount of each dye. To get the total number of emitted photons for each dye, it is necessary to have lifetime measurements done in the mixtures. The lifetimes of dyes were measured separately and then in mixtures:

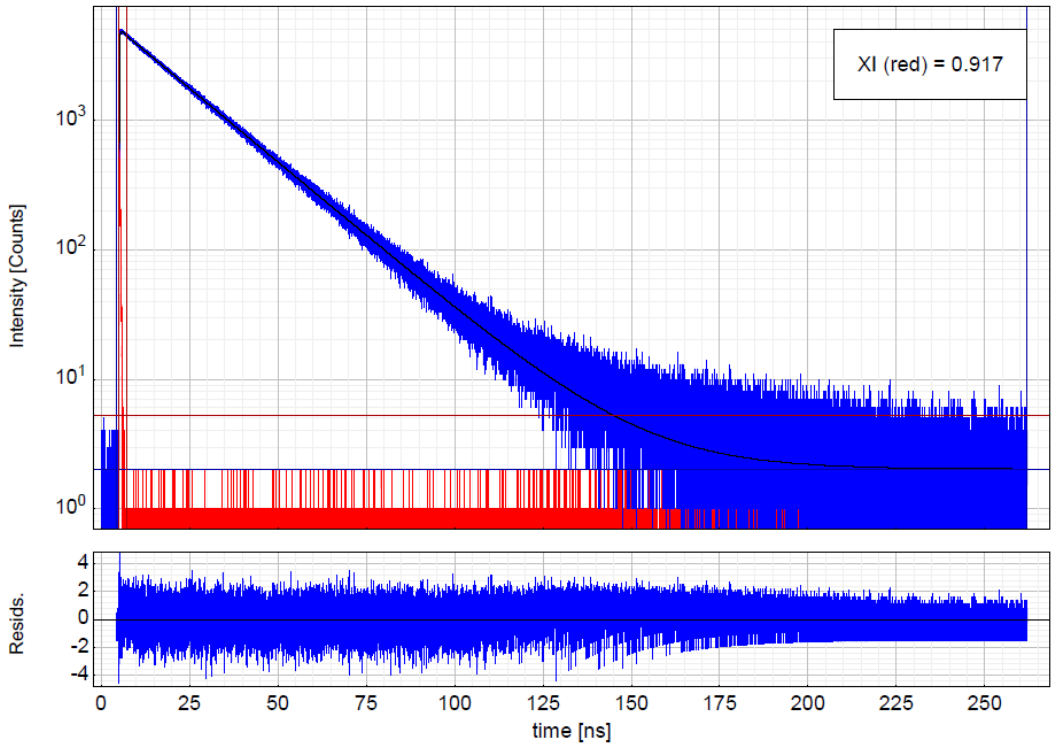

Parameter	Value	Conf. Lower	Conf. Upper	Conf. Estimation
A_1 [Cnts]	5212.9	-41.4	+41.4	Fitting
τ_1 [ns]	19.062	-0.111	+0.111	Fitting
Bkgr. Dec [Cnts]	2.024	-0.405	+0.405	Fitting
Bkgr. IRF [Cnts]	5.29	-2.04	+2.04	Fitting
Shift IRF [ns]	-0.02280	-0.00778	+0.00778	Fitting

Figure 15. Intensity decay of DAOTA fitted with a single exponential model

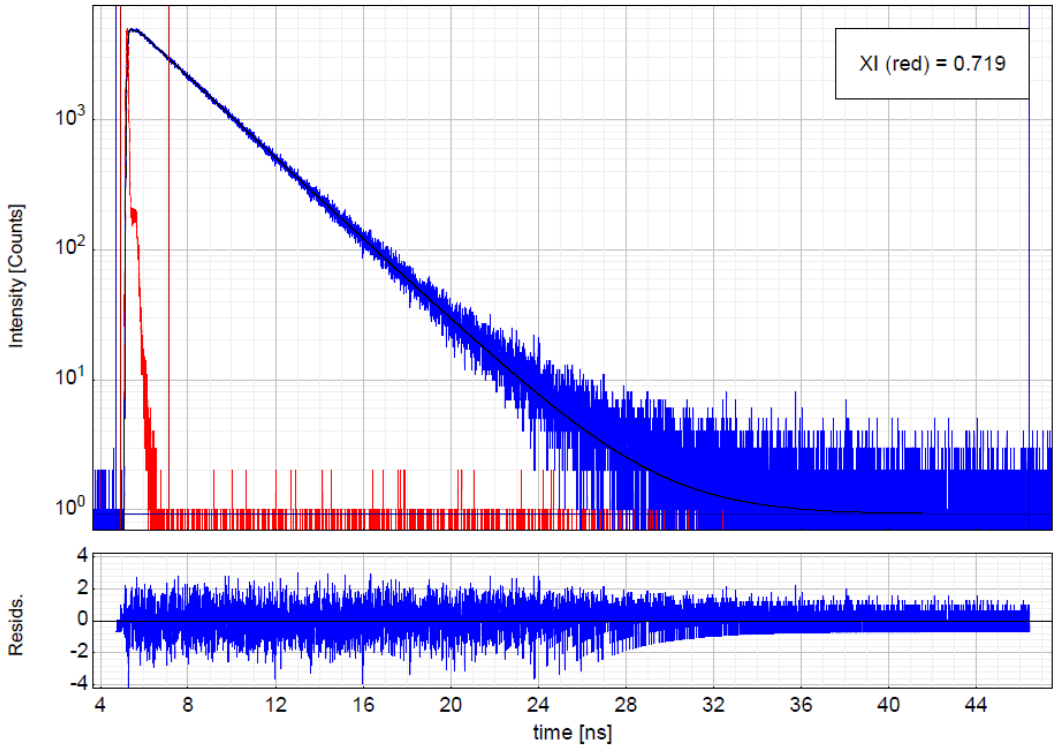

Parameter	Value	Conf. Lower	Conf. Upper	Conf. Estimation
A_1 [Cnts]	5926.8	-40.8	+40.8	Fitting
τ_1 [ns]	2.7830	-0.0139	+0.0139	Fitting
Bkgr. Dec [Cnts]	0.922	-0.294	+0.294	Fitting
Bkgr. IRF [Cnts]	0.65	-1.49	+1.49	Fitting
Shift IRF [ns]	-0.00937	-0.00263	+0.00263	Fitting

Figure 16. Intensity decay of RhB fitted with a single exponential model

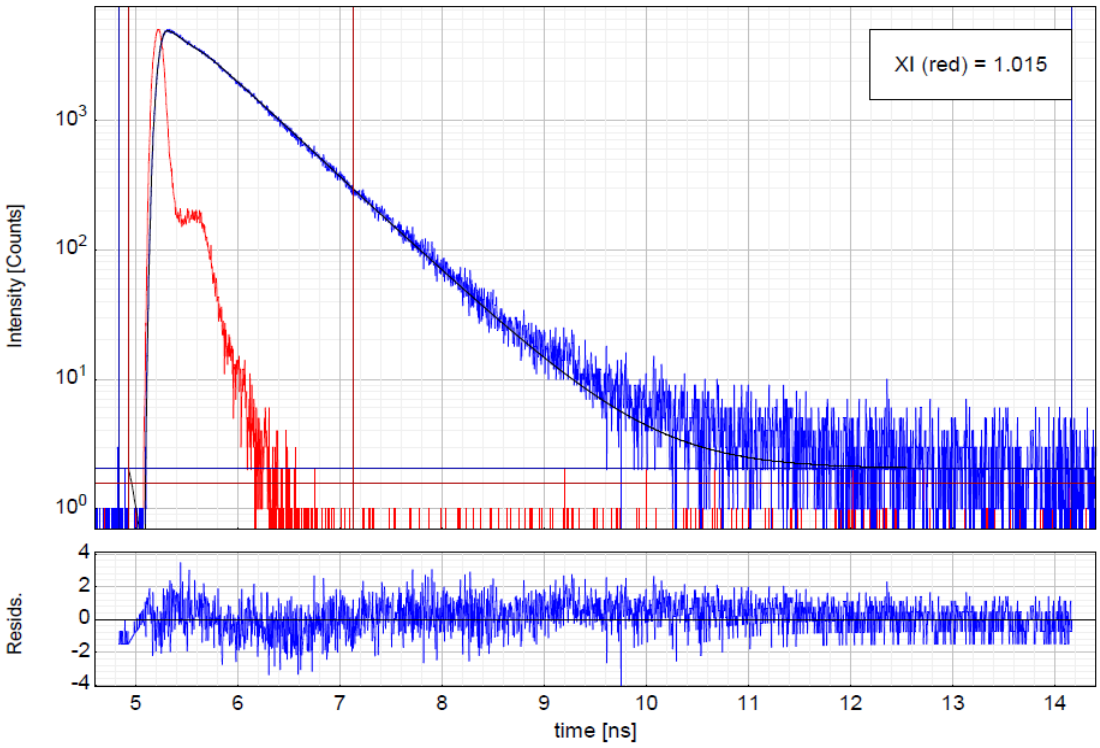

Parameter	Value	Conf. Lower	Conf. Upper	Conf. Estimation
A_1 [Cnts]	6915.6	-53.6	+53.6	Fitting
τ_1 [ns]	0.59607	-0.00337	+0.00337	Fitting
Bkgr. Dec [Cnts]	2.046	-0.408	+0.408	Fitting
Bkgr. IRF [Cnts]	1.58	-1.12	+1.12	Fitting
Shift IRF [ns]	-0.01061	-0.00141	+0.00141	Fitting

Figure 17. Intensity decay of ErB fitted with a single exponential model

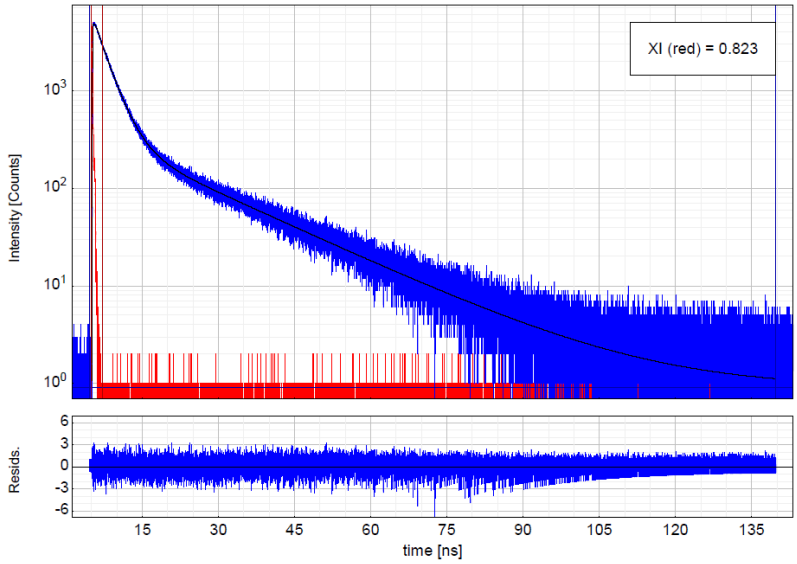

Parameter	Value	Conf. Lower	Conf. Upper	Conf. Estimation
A_1 [Cnts]	5487.3	-84.3	+84.3	Fitting
τ_1 [ns]	2.6502	-0.0354	+0.0354	Fitting
A_2 [Cnts]	361.43	-9.70	+9.70	Fitting
τ_2 [ns]	18.175	-0.324	+0.324	Fitting
Bkgr. Dec [Cnts]	0.904	-0.377	+0.377	Fitting
Bkgr. IRF [Cnts]	-0.055	-3.73	+3.73	Fitting
Shift IRF [ns]	-0.01034	-0.00529	+0.00529	Fitting

Figure 18 (a). Intensity decay of DAOTA and RhB fitted with a two-exponential model

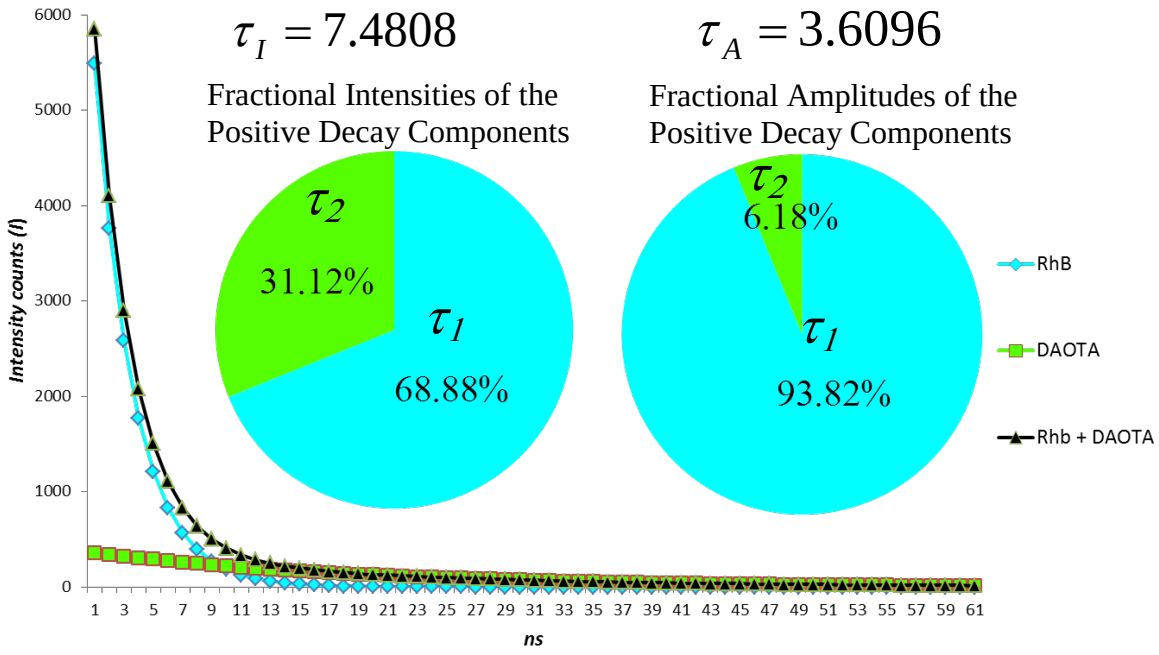

Figure 18 (b). Fractional intensities and amplitudes relationships are expressed with pie diagrams; intensity and amplitude weighted lifetimes are denoted by τ_A and τ_I, separated decays and their sum is plotted in the bottom

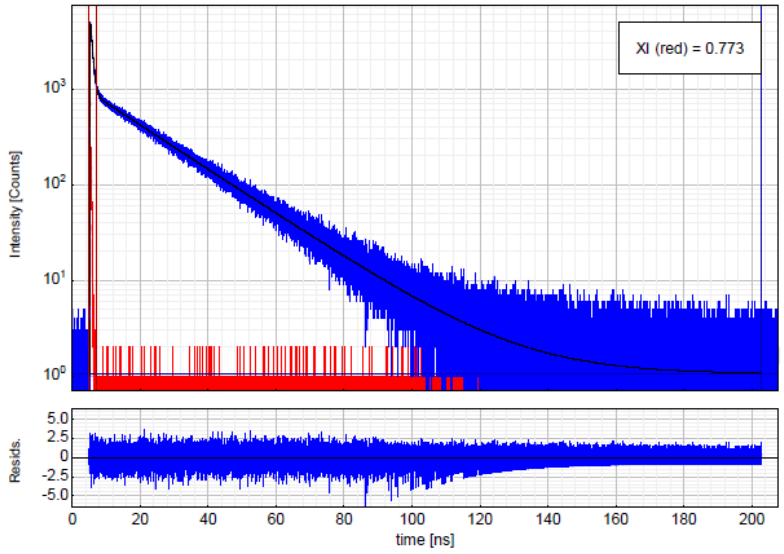

Parameter	Value	Conf. Lower	Conf. Upper	Conf. Estimation
A_1 [Cnts]	5720	-240	+240	Fitting
τ_1 [ns]	0.5830	-0.0250	+0.0250	Fitting
A_2 [Cnts]	957.2	-14.8	+14.8	Fitting
τ_2 [ns]	18.691	-0.216	+0.216	Fitting
Bkgr. Dec [Cnts]	1.052	-0.327	+0.327	Fitting
Bkgr. IRF [Cnts]	0.130	-5.32	+5.32	Fitting
Shift IRF [ns]	-0.01160	-0.00609	+0.00609	Fitting

Figure 19 (a). Intensity decay of DAOTA and ErB fitted with a double exponential model

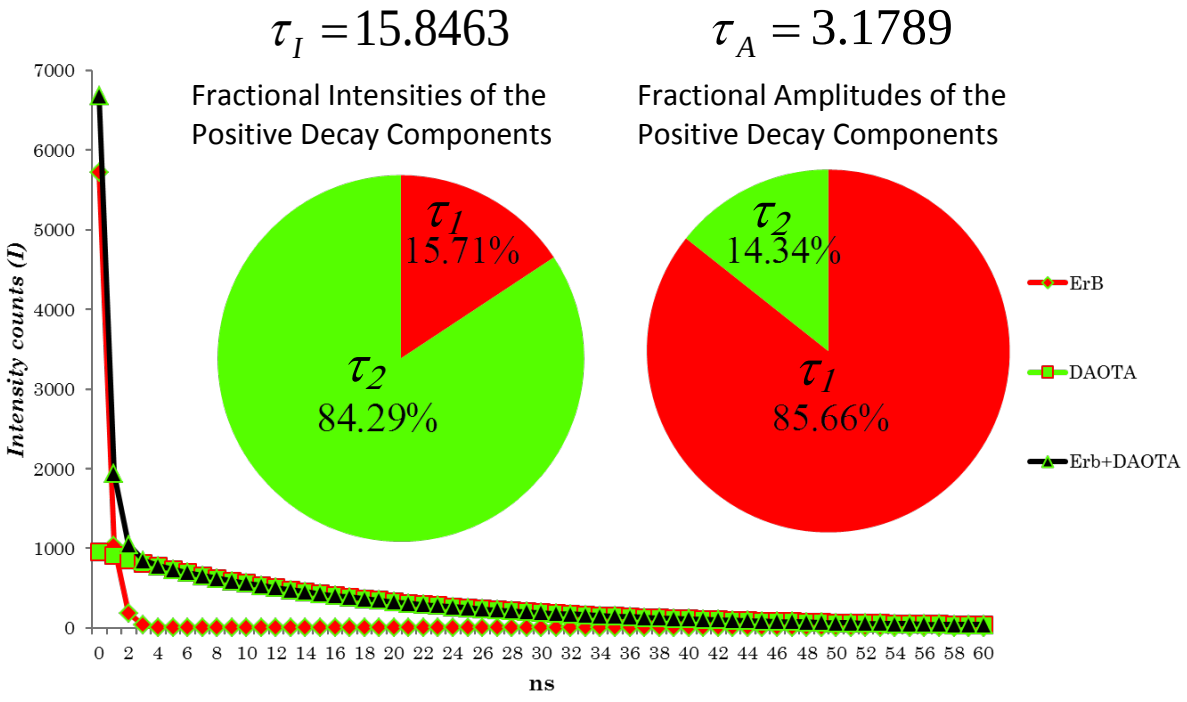

Figure 19 (b). Fractional intensities and amplitudes relationships are expressed with pie diagrams; intensity and amplitude weighted lifetimes are denoted by τ_A and τ_I, separated decays and their sum is plotted in the bottom

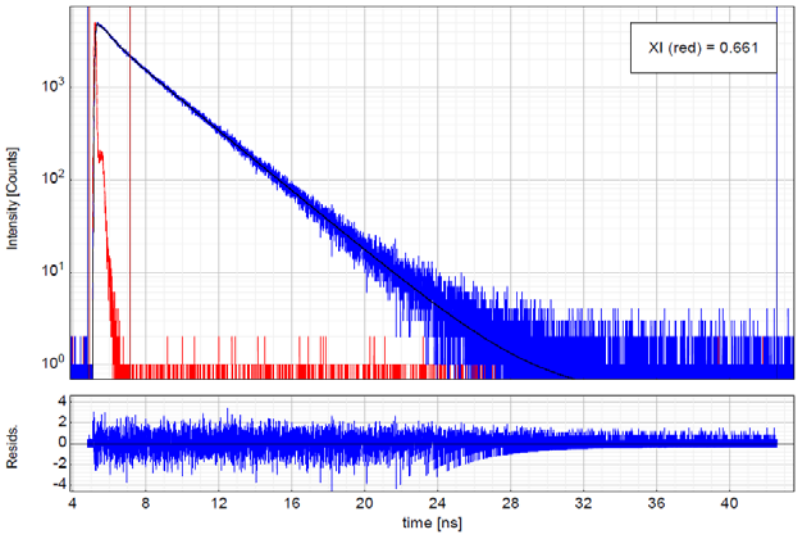

Parameter	Value	Conf. Lower	Conf. Upper	Conf. Estimation
A_1 [Cnts]	4366.5	-33.9	+33.9	Fitting
τ_1 [ns]	2.6777	-0.0145	+0.0145	Fitting
A_2 [Cnts]	1893	-106	+106	Fitting
τ_2 [ns]	0.5881	-0.0388	+0.0388	Fitting
Bkgr. Dec [Cnts]	0.468	-0.268	+0.268	Fitting
Bkgr. IRF [Cnts]	0.197	-1.96	+1.96	Fitting
Shift IRF [ns]	-0.00864	-0.00233	+0.00233	Fitting

Figure 20 (a). Intensity decay of RhB and ErB fitted with a double exponential model

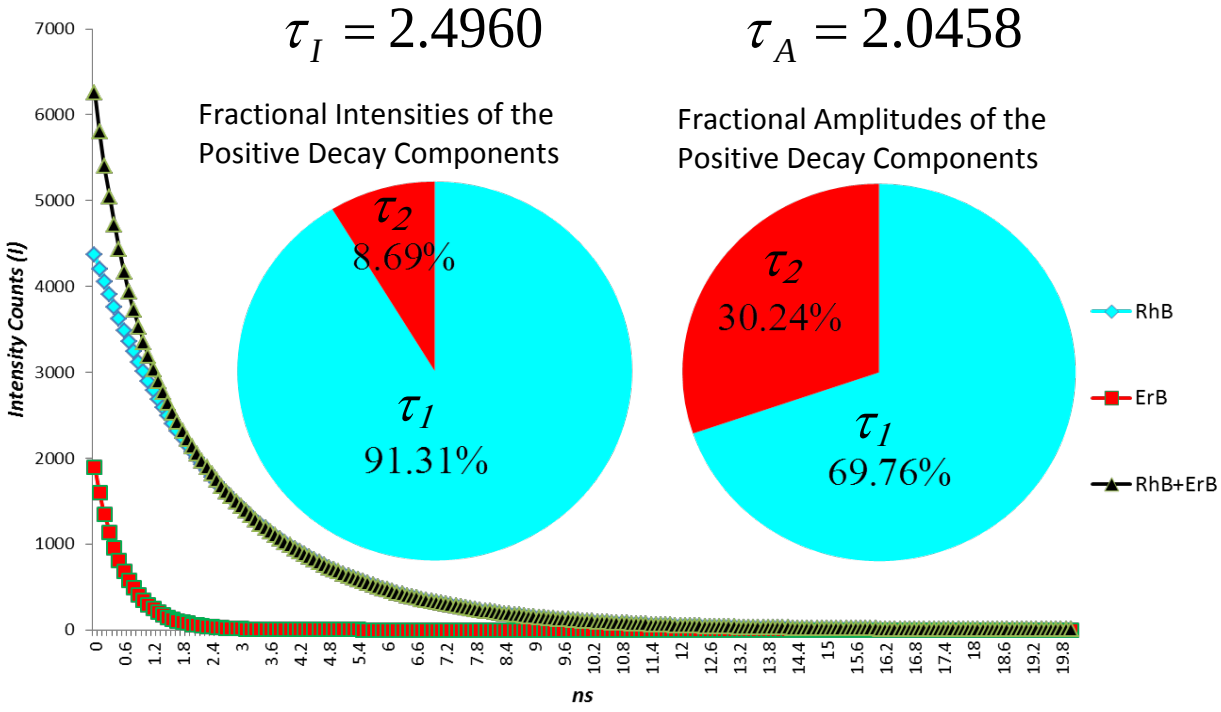

Figure 20 (b). Fractional intensities and amplitudes relationships are expressed with pie diagrams; intensity and amplitude weighted lifetimes are denoted by τ_A and τ_I, separated decays and their sum is plotted in the bottom

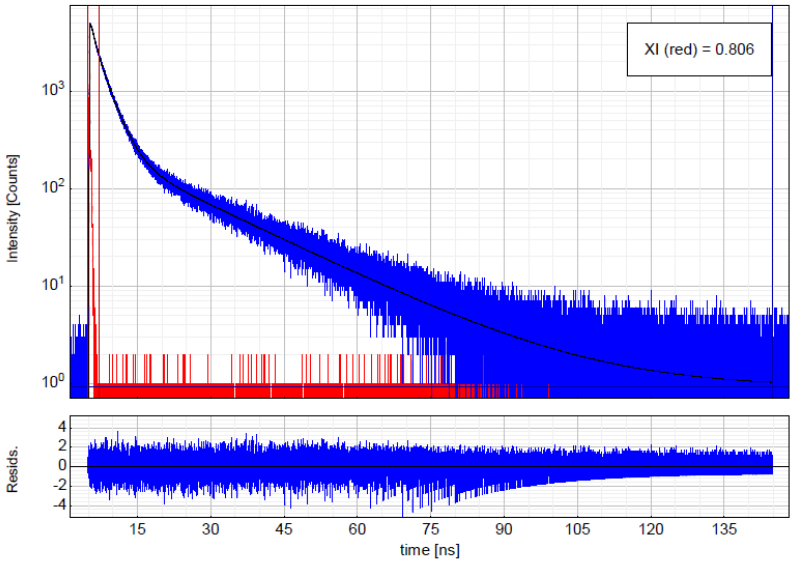

Parameter	Value	Conf. Lower	Conf. Upper	Conf. Estimation
A_1 [Cnts]	4386.7	-79.5	+79.5	Fitting
τ_1 [ns]	2.5839	-0.0395	+0.0395	Fitting
A_2 [Cnts]	277.13	-8.65	+8.65	Fitting
τ_2 [ns]	17.936	-0.382	+0.382	Fitting
A_3 [Cnts]	1588	-235	+235	Fitting
τ_3 [ns]	0.5596	-0.0996	+0.0996	Fitting
Bkgr. Dec [Cnts]	0.918	-0.343	+0.343	Fitting
Bkgr. IRF [Cnts]	0.60	-4.38	+4.38	Fitting
Shift IRF [ns]	-0.01070	-0.00514	+0.00514	Fitting

Figure 21 (a). Intensity decay of RhB, DAOTA and ErB fitted with a three component model

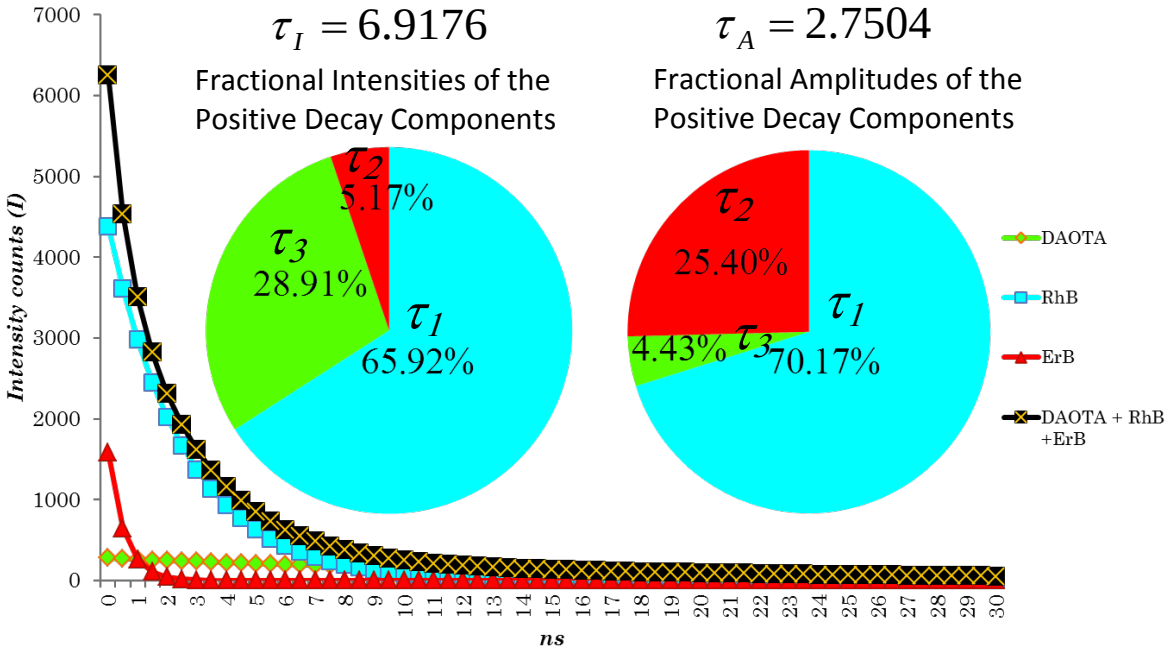

Figure 21 (b). Fractional intensities and amplitudes relationships are expressed with pie graphs, intensity and amplitude weighted lifetimes are denoted by τ_A and τ_I, separated decays and their sum are ploted in the bottom

Lifetimes were collected at the wavelength of 575 nm. Figures 15-17, 18 (a), 19 (a),20 (a) and 21 (a) represent lifetimes of each dye and their mixtures. Mixtures' decays are fitted with two or three component exponential decays $I = \Sigma_n I_{n0} e^{-t/\tau}$. Tables under the graphs contain initial amplitude of the decay for each dye A_i (later denoted as $I_{i)}$ and lifetimes τ_t. Background counts that are subtracted by software. Shift of the instrument response function (IRF) is done by software too, because photons of different wavelength may be differently delayed in the systems.

Each exponential decay represents a dye participating in the multi-exponential decay of the mixture. Fractional amplitudes in Figures 18, 19, 20 and 21 give relationships between the number of photons emitted by each dye at t = 0, fractional intensities give the relationship between the number of photons going through all the time channels [23]. Figures that represent multi-exponential decays, contain a plot of each decay and their sum on the bottom of the figure. Fractional amplitudes and intensities of decay components are calculated using formulas:

$$fA_i = \frac{I_i}{\sum_j I_j} \qquad fI_i = \frac{I_i \tau_i}{\sum_j I_j \tau_j} \tag{23}$$

where I_i stands for intensity of the particular fraction (dye), $\Sigma_j I_j$ is the sum of all the fractions (dyes) and τ_t is the lifetime of each function. Intensity average lifetime is the average lifetime of a collection of the different intensity decays (dyes) presented in the solution. Amplitude average lifetime defines the lifetime that fluorophore would have if it has the same emission properties as a set of a few dyes. Amplitude weighted average and intensity weighted average lifetimes are calculated using formulas:

$$< \tau_A >= \sum_{i=1}^{n} \frac{fA_i \tau_i}{fA_i} \qquad < \tau_I >= \sum_{i=1}^{n} \frac{fA_i \tau_i^2}{fA_i \tau_i} \tag{24}$$

Note that the dimer and monomer form of AO have different lifetimes. The lifetime of a dimer is around 20 ns; the lifetime of a monomer is around 1.5 ns, so a decrease of concentration can be monitored by fractional amplitudes and intensities changes.

ACRIDINE ORANGE (AO) MEASUREMENTS RESULTS, DISCUSSION

Absorption

Stock solution of AO at a concentration of 28 g/L was prepared using deionized water and AO. Absorption measurements for a high concentration (28 g/L) were performed in the following way. On a Menzel microscopy slide we drew a square with a vacuum grease marker, then 1.5 μL of solution was put on the square and covered with another slide, producing a "sandwich". A different slide with water instead of a sample was prepared for blank measurements. Low concentrations of AO with no dimers (0.005 g/L) were measured in a 1 mm cuvette. Some concentrations were measured both in a slide and in a cuvette to control consistence of measurements. Measurements were performed on the Agilent Technologies 8453 absorption spectrometer. High concentrations of the AO were not measured in the cuvette, because the light from the lamp was able to penetrate only few millimeters deep in the sample.

Absorption spectra for AO concentrations of 0.025, 0.0025 g/L were measured in a cuvette. Concentrations 28, 14, 4, 1, 0.2 g/L were measured with the technique that uses two microscopy slides. Spectra were normalized and plotted (Figure 22).

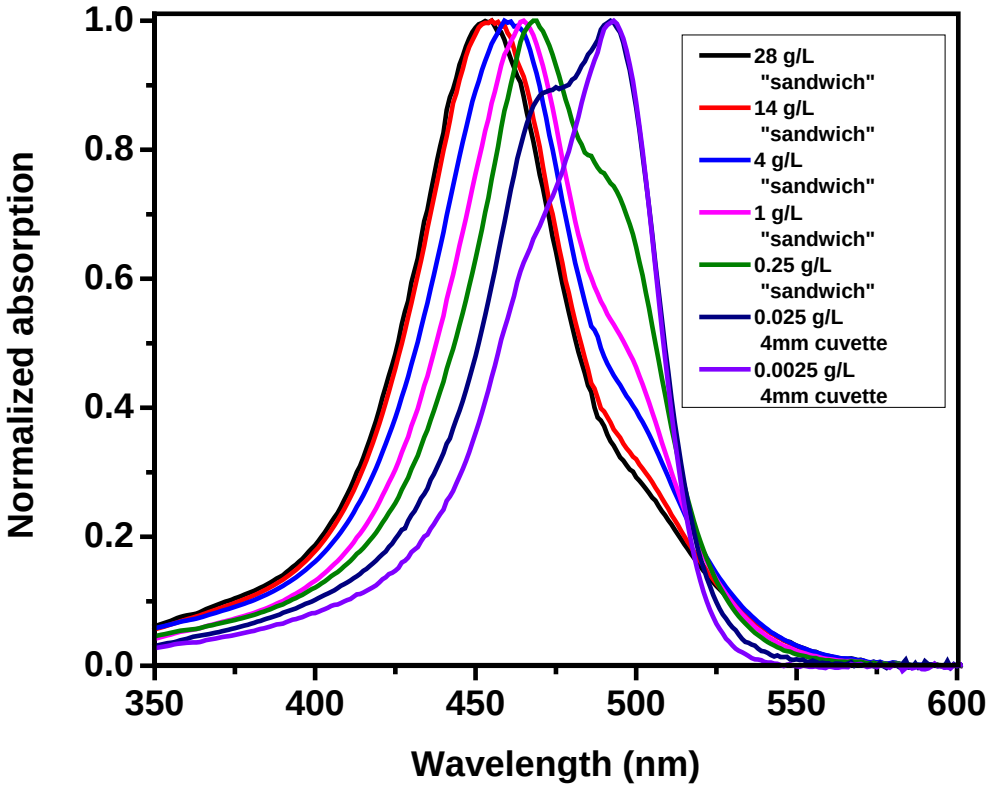

Figure 22. Absorption spectra of AO

In Figure 22 one can see that a decrease in concentration corresponds to an increase of the monomeric form in the solution. A concentration of 4 g/L already shows a “shoulder” around 490 nm, which is due to the monomeric form absorption maximum. Further decrease of the concentration leads to only one absorption peak that represents the monomeric form. The absorption peak of the dimer form shifts to longer wavelengths.

Emission Spectra and Lifetimes

Standard square geometry cuvette measurements were not applicable in this case because at high concentrations almost all photons were absorbed within few microns (Figure 23):

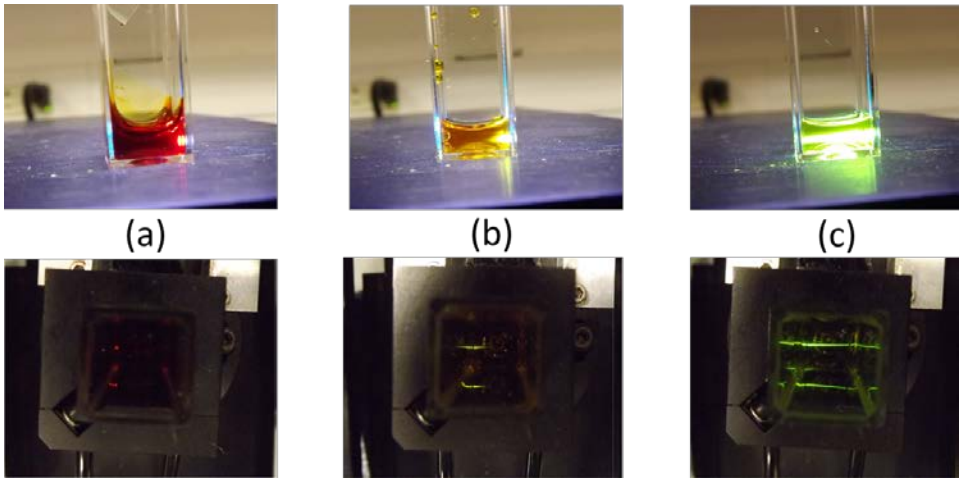

Figure 23. Propagation of 494nm excitation through the cuvettes with different AO concentration. (a) 28g/L, (b) 0.5g/L, (c) 0.05g/L

Emission spectra for high concentrations were collected using the front face setup developed in our lab (Figure 24).

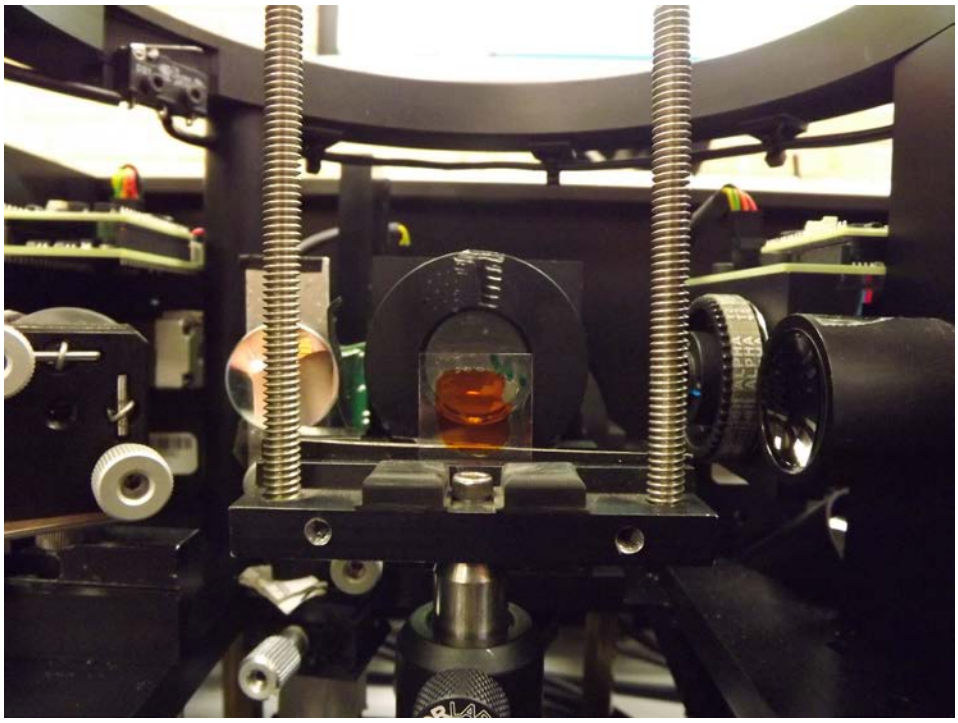

Figure 24. Front face setup in FT300's chamber with AO 28g/L "sandwich".

The front face setup allowed us to measure high concentrations of AO and prevents the influence of reabsorption's effect on the measurements. Lifetimes were also measured in this configuration. Low concentration measurements (monomer form dominance) required larger volumes to have reasonable signal to noise ratio. To prevent reabsorption influence, in square geometry measurements were performed in a special setup, which allows excitation on the very edge of the cuvette (Figure 25):

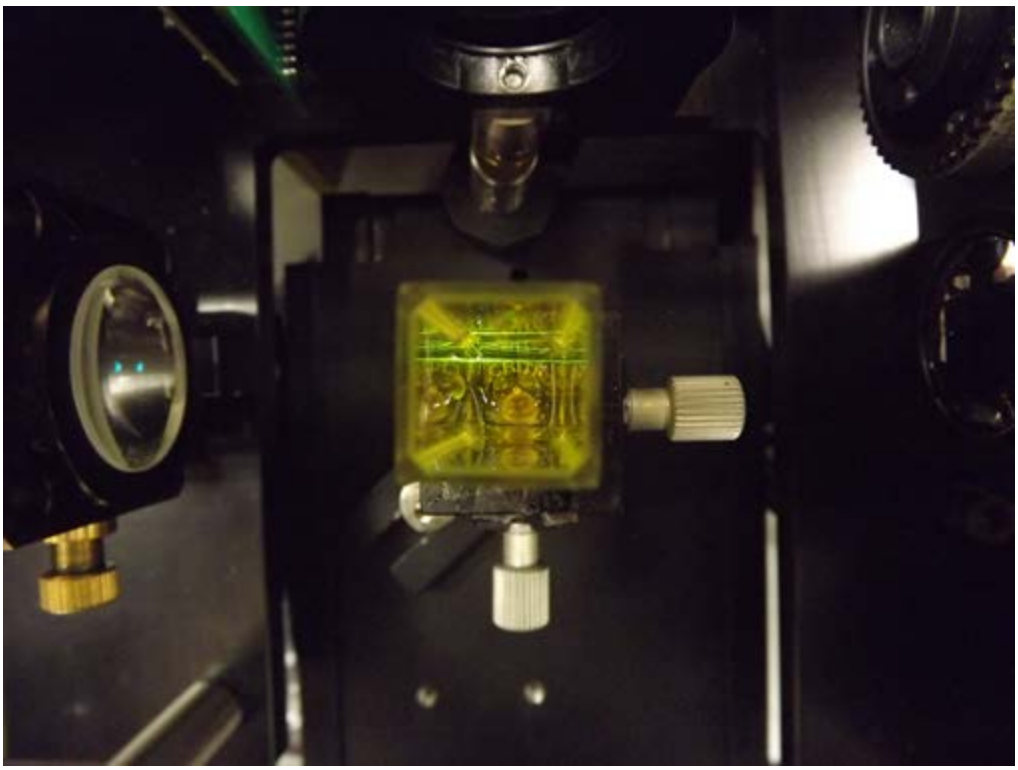

Figure 25. Excitation of 0.05g/L concentration on the edge of the cuvette

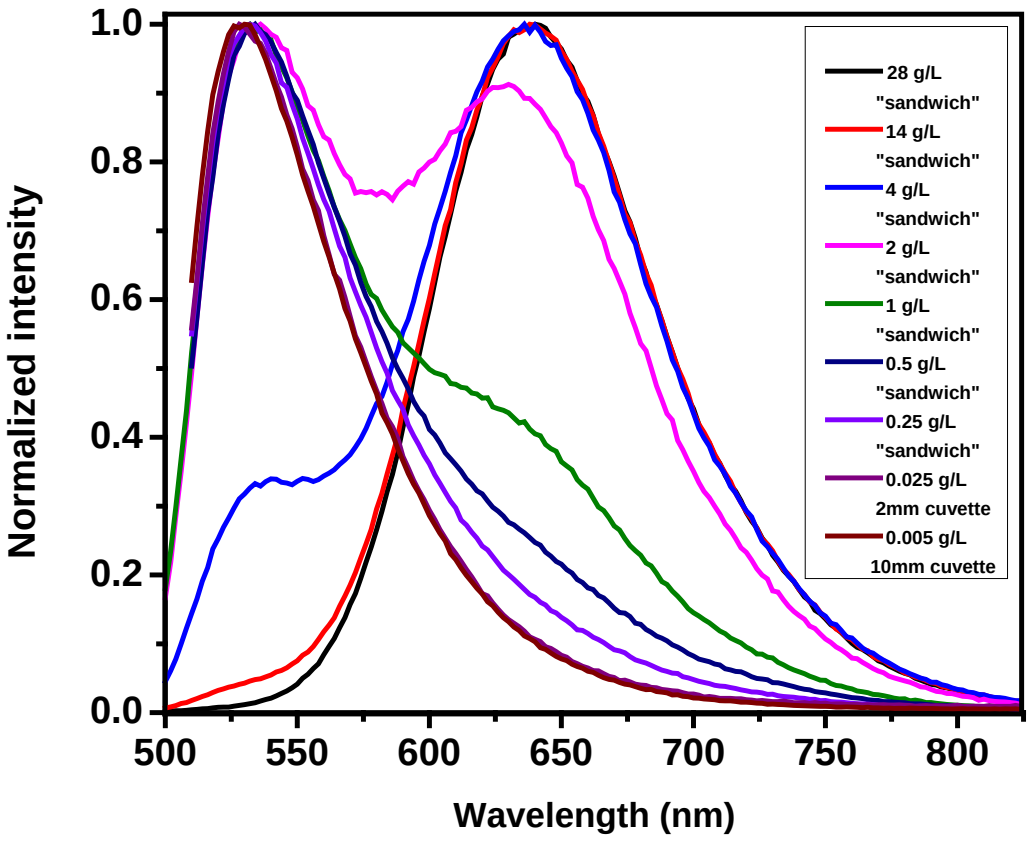

Figure 26. Normalized emission spectra of AO with 494nm excitation wavelength

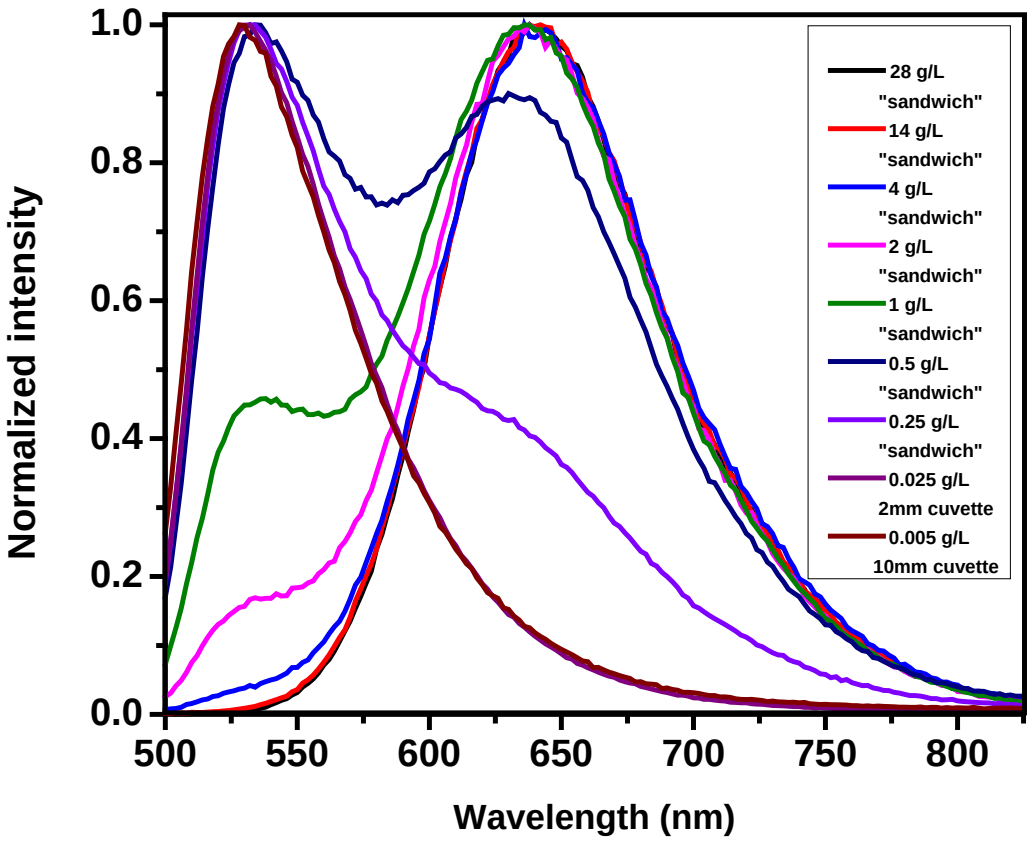

Figure 27. Normalized emission spectra of AO with 435nm excitation wavelength

Emission spectra for concentrations of 28, 14, 4, 2, 1, 0.5, 0.25, 0.025, 0.005 g/L were measured with excitations 435 and 494 nm. These wavelengths were selected to excite mainly one form and minimize excitation of another. Excitation with wavelength of 435 nm was performed for the dimer, and excitation with wavelength of 494 nm was done for the monomer. Spectra were normalized and plotted in Figures 26, 27. By analyzing emission spectra one can see that the highest concentration of 28 g/L has only one peak with the maximum around 640 nm for both excitation wavelengths. Concentration of 14 g/L with excitation wavelength of 494 nm produces a small “bump” around 530 nm, which is the signature of the monomer form; it means that the monomeric form is already present in the solution. Further decrease of concentration

causes the monomeric peak to grow and then completely dominate the emission spectra. At very low concentrations (0.05 - 0.0005 g/L) only monomers can be detected. Absorption peak at 435 nm belongs mostly to the dimer, but the monomer is excited too.

Extinction Coefficient

Decadic molar extinction coefficient describes how strongly a molecule absorbs light at a certain wavelength. Decadic molar extinction coefficient can be determined from the Beer-Lambert law if absorption, concentration and sample thickness are known. Low concentrations of AO (starting with 0.05 g/L) can be measured in a cuvette with known thickness. However, higher concentrations cause saturation, because excitation light penetrates only a few microns. To determine the decadic molar extinction coefficient the following procedure was implemented: a similar "sandwich" as for the emission spectra and lifetime measurements was prepared using 5 μL of 28 g/L AO solution. (See below: its picture taken with digital camera Fujitsu FinePix S4000, Figure 28)

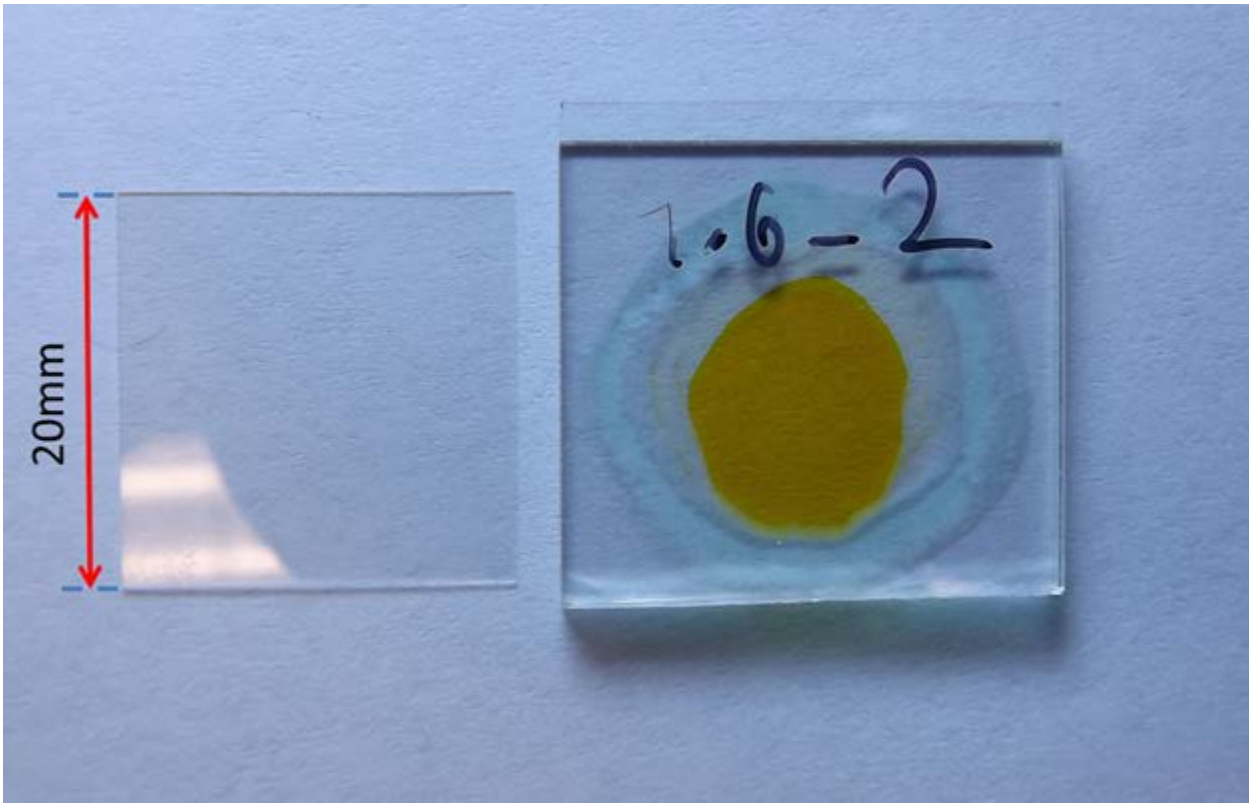

Figure 28. Picture of the AO slide

Absorption of the “sandwich” was greater than 1.5 O.D., as expected, and our instrument could not resolve all needed wavelengths, especially near the absorption peak, see Figure 29. It was decided to perform measurements for the highest thickness that our instrument could resolve. A drop of AO solution was measured between two microscopy slides that were squeezed together to achieve smallest possible thickness of the solution layer in between.

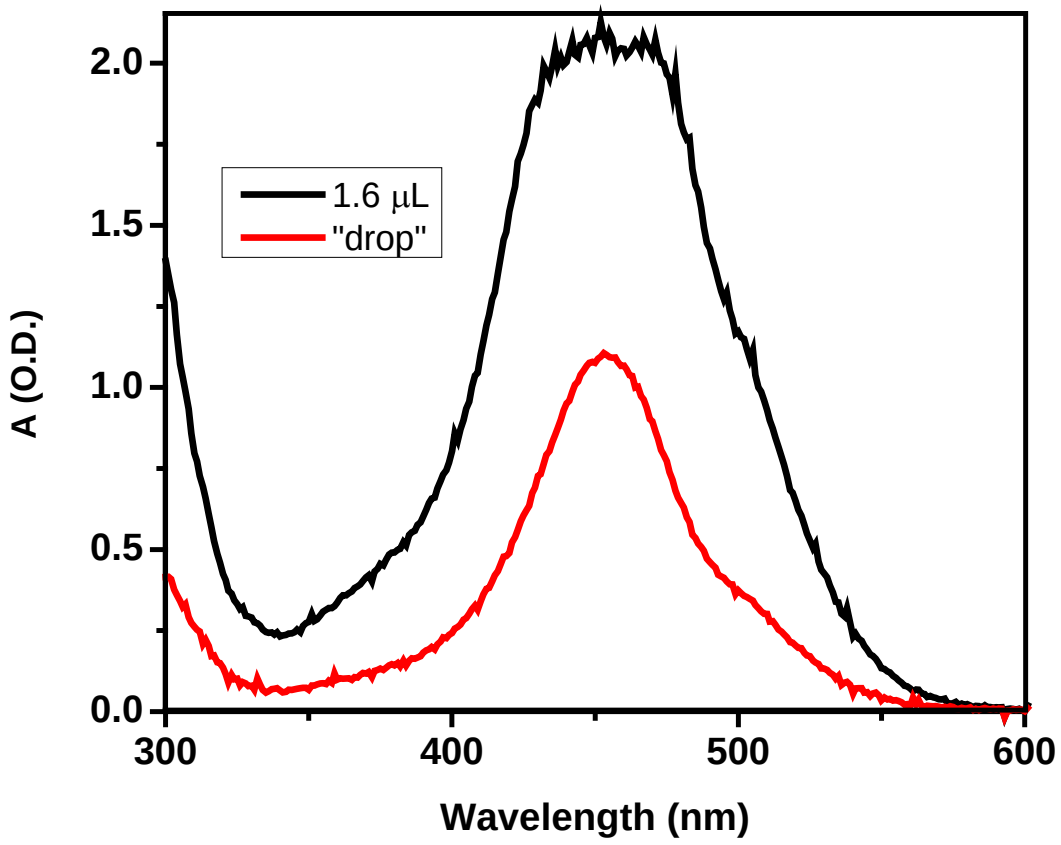

Figure 29. Absorption of 10μL “sandwich” and a drop of 28g/L AO solution

Absorption at the peak was recalculated, taking into account the fact that it should be proportional for all wavelengths, for both the small and large path lengths. The ratio of absorption of a “sandwich” and a “drop” is constant at all wavelengths. Using Adobe Photoshop

software it was possible to determine the exact area filled by the solution and knowing the volume one could recalculate the thickness. The region of “sandwich” with a dye (sample area) was selected, using its color. The extinction coefficient for the dimer at 460 nm wavelength (28 g/L) was calculated to be 43000+/-1000 $M^{-1}cm^{-1}$in a 7.4 pH 0.5 M phosphate buffer. Extinction coefficients of AO were measured before [14] and are found in literature, but not for the saturated solution. Extinction coefficient of the monomer has been estimated from low concentration measurement to be (for concentration of 0.005 g/L) 15000+/-1000 $M^{-1}cm^{-1}$.

Quantum Yield Measurements

Quantum yield (Q) is an important property of all fluorescent dyes, as it defines the probability of photon emission and dictates overall brightness of the dye. We did Q measurements of the dimers and monomers using reference dyes with the similar emission properties. AO dimer, dissolved in water, has the emission peak around 640 nm and the absorption maximum around 460 nm. Excitation wavelength of 435 nm was selected to prevent excitation of the monomer form. Tris(bipyridine)ruthenium(II) chloride was used as a reference dye for Q measurements. It can be excited at 435 nm and emits around 640 nm. Then quantum yield was calculated, using the formula [24,25]:

$$Q_{AO} = Q_{RU} \frac{I_{AO}}{I_{RU}} \frac{N_{RU}}{N_{AO}} \frac{n_{RU}^2}{n_{AO}^2} \tag{32}$$

where Q_{AO} and Q_{RU} are the quantum yields of acridine orange(AO) and Ruthenium respectively. I_{AO}, N_{AO} is intensity and number of absorbed photons for AO, I_{RU}, N_{RU} are intensity and number of absorbed photons for Ruthenium; and n_{RU} and n_{AO} are the corresponding refractive indexes of solvents that were used for sample preparation. Ruthenium was dissolved in ethanol, AO in water. Here intensity is considered to represent the total number of emitted photons by the dye and was calculated as a sum of counts for all the wavelengths. Ruthenium's quantum yield is 0.02. For the monomer form with absorption maximum around 495 nm and emission 530 nm, Uranin was used as a reference dye. Q of dimer (28 g/L) was calculated to be 0.015 +/-0.002. Q of the monomer (0.005 g/L) was calculated to be 0.155+/-0.003.

Acridine Orange (AO) Lifetime Measurements

Emission spectra show a clear dependence of AO emission properties on the concentration. Fluorescence lifetime measurements will also provide information about the concentration of AO but independently of the signal level and signal perturbation from the cellular environment. Lifetime measurements were performed for a range of concentrations, where a change in dimer/monomer equilibrium was expected to be observed. The measurements were done with FT 300 system using Fianium SC 400-4-PP super continuum laser with 435 nm and 494 nm excitation wavelengths, selected by band path filters. Figure 30 and Figure 31 represent AO lifetime measurements (intensity decays) performed for selected concentrations:

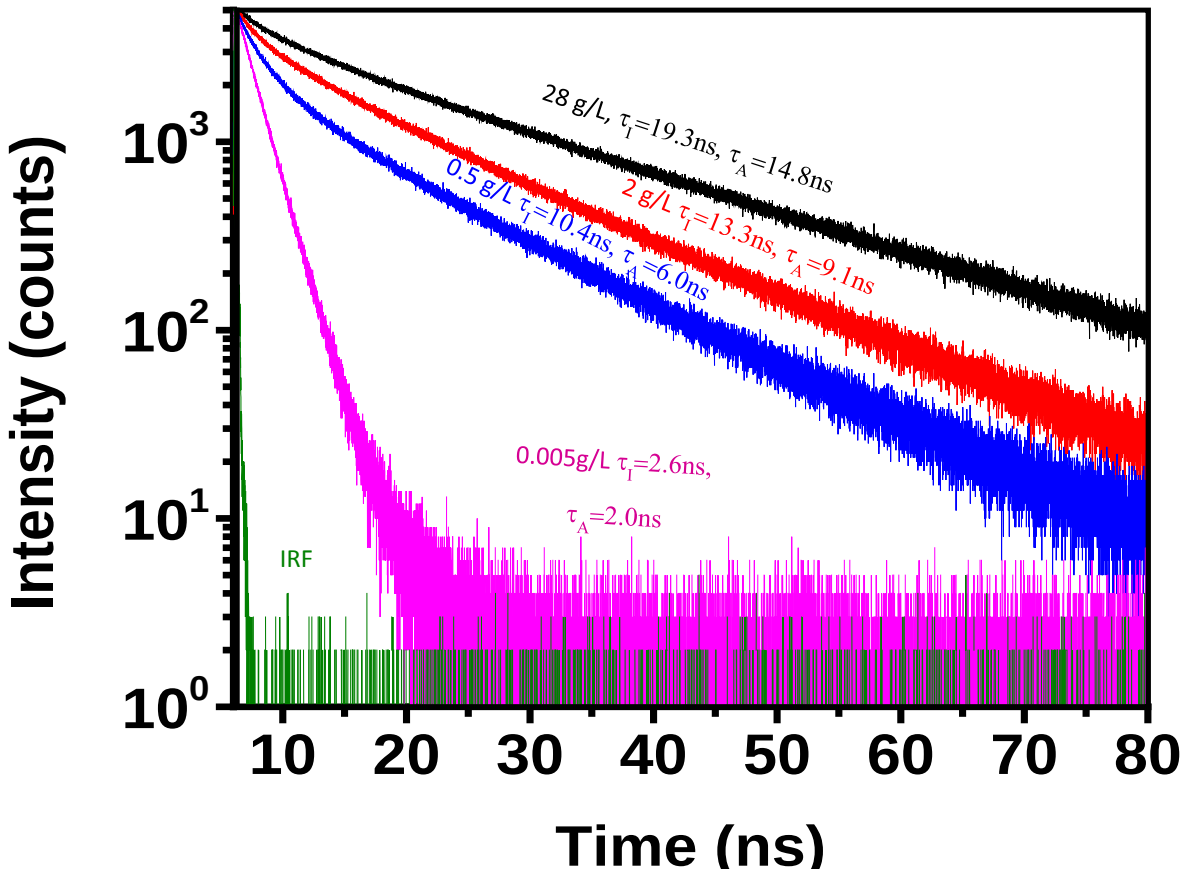

Figure 30. Intensity decays of AO with 435nm excitation wavelength, 640nm emission wavelength, intensity and amplitude averaged lifetimes

Two sets of measurements were performed in correspondence with excitation wavelengths of 435 nm and 494 nm, and with 640 nm emission wavelength where monomers and dimers emit respectively.

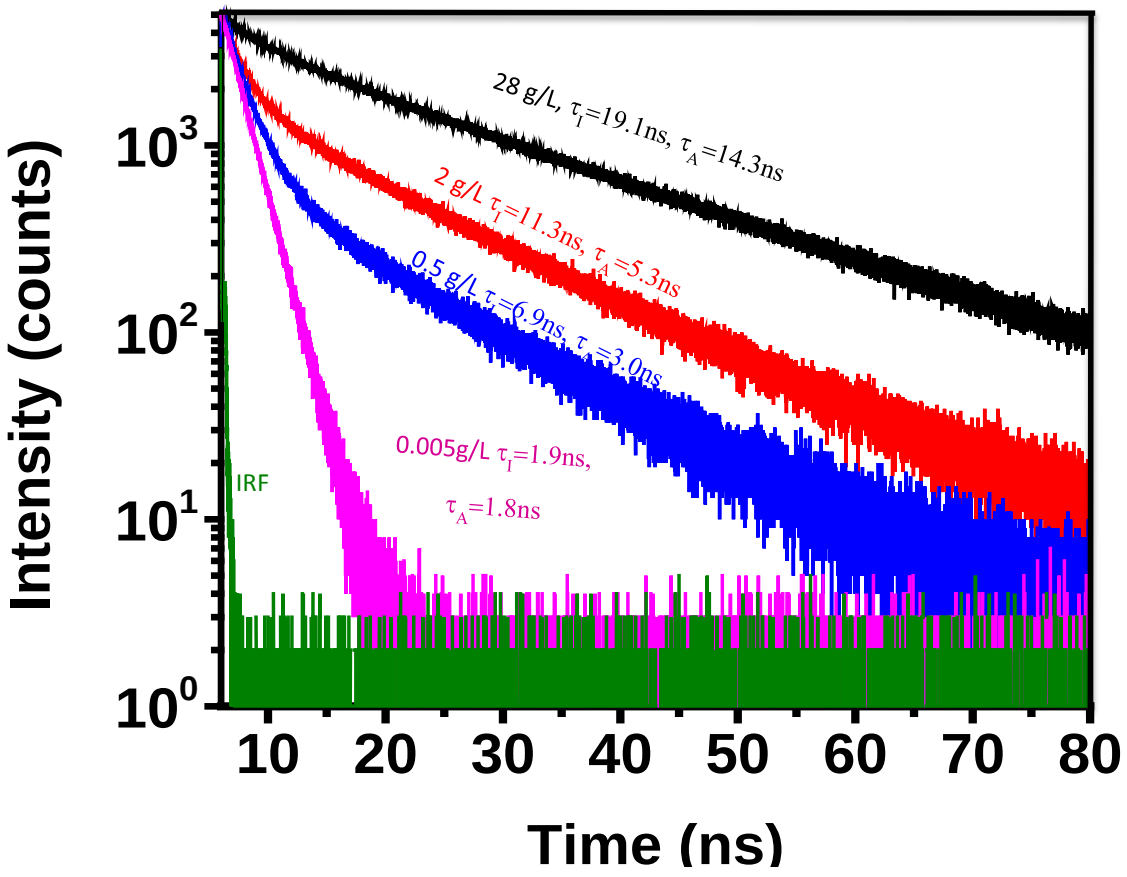

Figure 31. Intensity decays of AO with 494nm excitation wavelength, 640nm emission wavelength, intensity and amplitude averaged lifetimes

Fluorescence lifetimes of dimers and monomers are different and we assumed that it would be possible to monitor concentration change of AO by fractional intensities and amplitudes changes, but results appeared to be more complex than it was expected. Data can only be fitted to the exponential function with 3 lifetime components: $I = \Sigma_n I_{n0} e^{-t/\tau}$, $n = 1, 2, 3$. Data fitting with more than 3 components typically does not make sense in lifetime measurements. So interaction of molecules at different concentrations and formation of intermediate species is possible, since we expected only single exponential decay for the monomers and aggregates. Intensity and amplitude averaged lifetimes can consequently provide some information about AO

concentration, especially the dataset with 435 nm excitation and 640 nm emission wavelengths, because changes in the intensity decays are not that rapid as with 494 nm excitation and 640 nm emission. The aggregate form is dominant at high concentration, its decay has mostly long component decay ~ 20 ns, monomeric form can be fitted with one component ~ 1.5 ns. From this it can be concluded that each form is represented by proper component and third component is due to interaction of two forms. However there is a shortening of the lifetime for both components with concentration change. Monitoring change of concentration as a function of component change can be a complex procedure, and since release of mucin containing granula and the mucin unfolding process lasts for a few hundreds of μs and it might be not be possible to get enough data for a statistically good fit. Because of this we will introduce a ratiometric technique, which will be described later.

TECHNIQUES FOR FUTURE EXPERIMENTS

Total Internal Reflection Fluorescence Microscope

Total internal reflection microscopy provides the possibility of studying fluorophores or fluorescently labeled molecules on the surface. An evanescence wave, which typically propagates a few hundred nanometers into the sample and experiences exponential decay, is created on the interface of two media with different refractive indices when an incident beam angle is lower than the critical angle. The refractive index of the initial medium has to be higher than that of the second medium.

One of the possible TIRF instrumental configurations in microscopy is to use special TIRF objectives. These objectives are designed in such a way, that the excitation beam is transferred from the back of the objective and can be adjusted at an angle lower than the critical angle, so total internal reflection conditions can be obtained. The scheme of a TIRF microscope is presented on Figure 33:

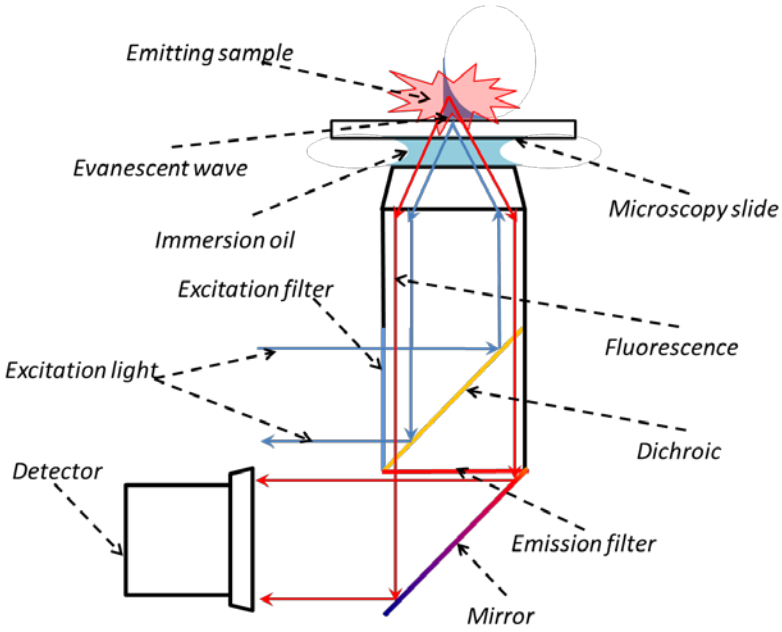

Figure 32. Scheme of TIRF microscope

Collection efficiency is high because the sample emits close to the focal point of the objective. Another advantage of microscope in fluorescence studies is possibility of acquiring an

image of the object in the focal plane using a CCD camera. Fluorescence lifetime imaging (FLIM) is also applicable in this particular configuration with the help of a scanning stage. [26,27]

Ratiometric Detection

We are going to introduce a ratiometric technique that is widely used in spectroscopy, but is not very popular in fluorescent microscopy. Ratiometric detection is based on the signal ratio from two different wavelengths or two different time points and is much less affected by the sample/signal perturbation, bringing an additional level of detection sensitivity/precision.

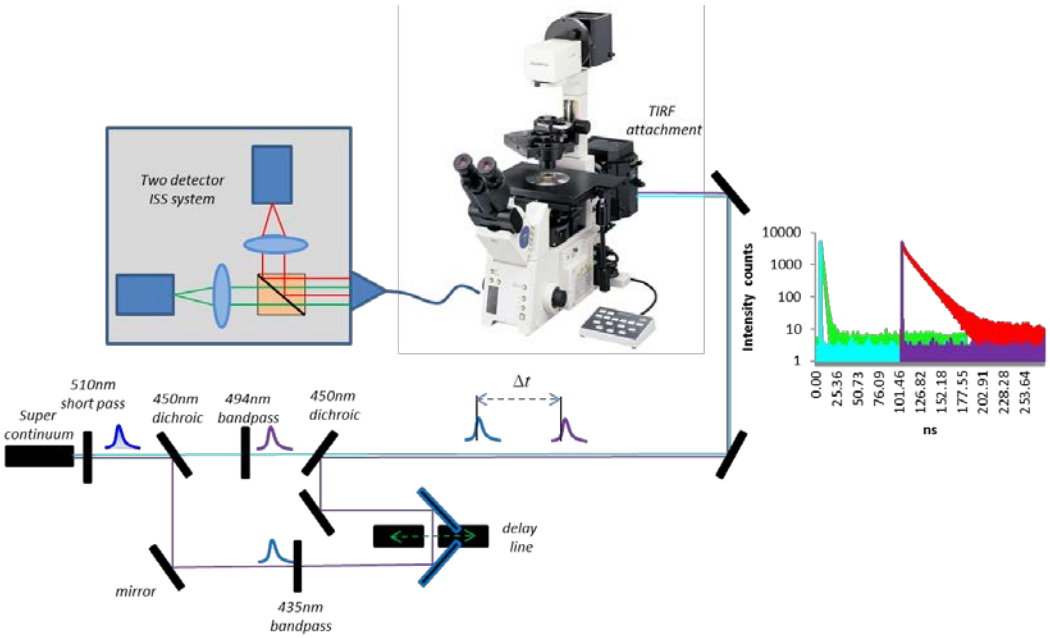

Figure 33. Schematic Configuration of TIRF with Dual Wavelength Excitation

We will be using detection at two different wavelengths. The monomeric form has an emission wavelength of 530 nm (green) and the aggregate emits at 640 nm (red). Collected emissions will be separated by a dichroic cube, as depicted on Figure 34, so each detector will be collecting decay of only one form. Software Vista Vision 4.0.00125 will be updated by ISS Company. New software will have the capability to resolve intensity decay from two detectors and automatically produce the ratio. Ratio of these decays will instantaneously determine theconcentration of AO, which can provide information about the volume increase of expanding mucins.

Future Experiments

Acridine orange released from vesicles, as well as mucin containing granules, will change its absorption and emission spectra as well as fluorescence lifetime. The change in absorption and emission spectra, and also in lifetimes creates an opportunity to perform using a ratiometric approach to precisely determine the concentration of AO in cells. We should be able to monitor processes in the ms range, during which mucus releases into the extracellular space. Results of the lifetime measurements of the granules and released mucins will provide data to obtain a numerical value for AO concentration change and mucin volume change. This study will help us understand the basic processes of mucin unfolding and formation of the mucus layer in lung epithelia. Application of TIRF will help us eliminate the background noise and provide the possibility of monitoring only a few 100 nm region, which is typically occupied by a membrane (Figure 34):

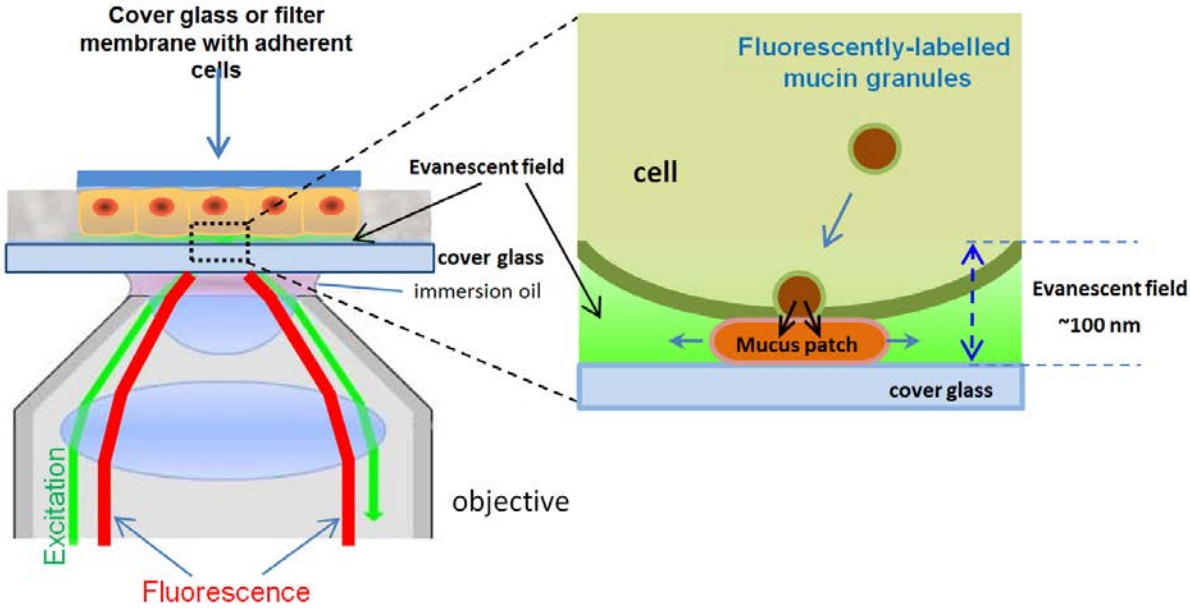

Figure 34. Scheme of Total Internal Reflection (TIR) microscopy applied for the study of mucus release process

Cell staining with AO will be performed in University of North Texas Health Science Center, where all needed equipment for cell incubation, preservation and staining is available. Cells will be grown on a glass substrate and put up – side - down with cells facing the glass bottom of the imaging chamber. Mechanical stimulation of the cells will be applied as was done in the preliminary experiments. Experiments will be conducted at 37°C.Healthy cells and Cystic Fibrosis like - Calu3 cells will be examined, and the difference between mucus release/formation processes in the two cell types will be determined.

Preliminary FLIM Experiments

Mucus release from epithelial cells is a process, characterized by vesicle formation in Golgi apparatus with further release of vesicle content into the intercellular space. Acridine Orange can accumulate in vesicles that have low pH (around 5.5). Mucus release causes mucins to unfold and increase in volume about a hundred times. Change of AO concentration can be monitored precisely with FLIM. Here we present an example of how fluorescence lifetime imaging can discriminate between objects that are not very different in their fluorescence intensities or transmissions. We took silica cluster, stained with Rhodamine, placed in ADOTA environment (PVA film containing ADOTA). Using TIR excitation [28] allows monitoring about 200 nm of sample depth, which separates the region near the surface from all other volume of the sample (Figure 35):

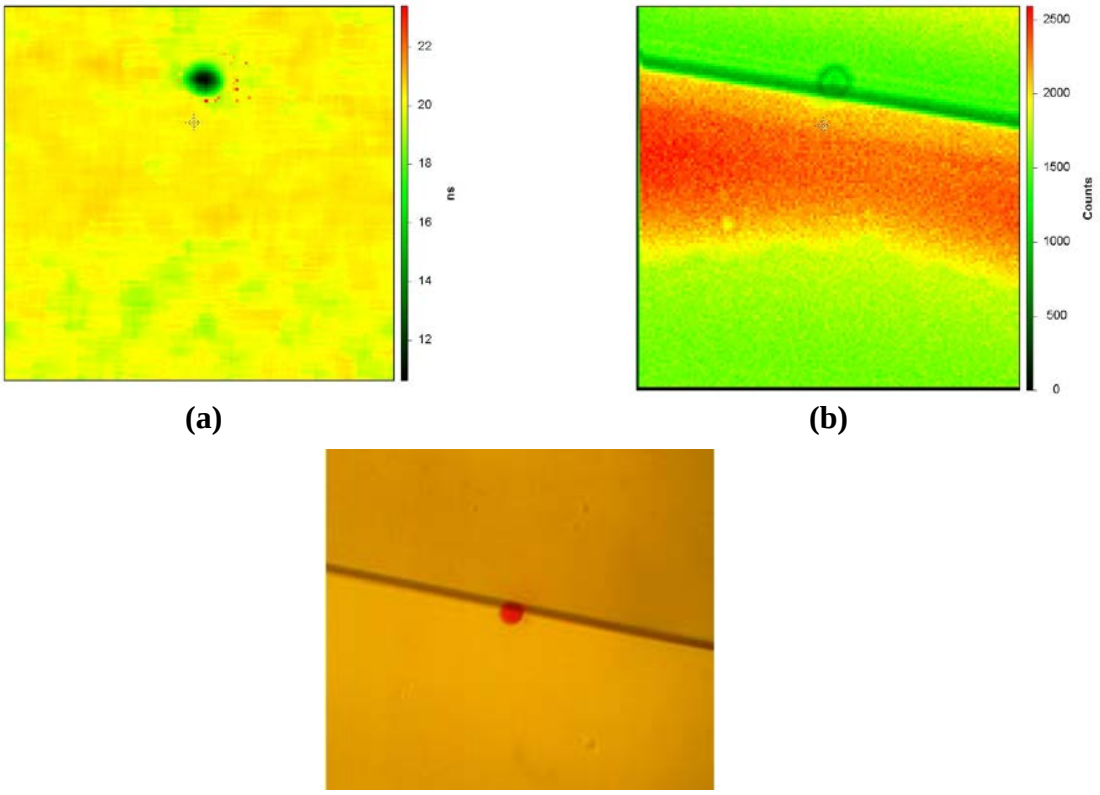

(a) **(b)**

(c)

Figure 35. (a) FLIM image, (b) intensity image, (c) CCD camera image with white light illumination

Images were collected in our laboratory with an X81 Olympus microscope, equipped with TIRF setup, 60X TIR objective and ISS two detector FLIM system. The system was adjusted to scan a region 100 μm by 100 μm with resolution of 128X128 pixels and integration time of 1 ms per pixel. A PicoQuant pulsed 487 nm laser diode was used to excite the molecules. The dark line is a scratch on a glass slide made for reference and easier objective focus adjustments. The CCD camera image represents the same picture as one is seeing with theeye. The intensity image illustrates intensity counts at each pixel. The FLIM image demonstrates the difference between space occupied by the bead and a free space.

Another experiment was conducted by Dr.Grygorczyk. Cells were stained with AO solution and lifetime images collected (Figure 36). It is possible to see that AO accumulates in thegranules of the epithelial cells (red region), also some AO molecules accumulate in the nucleus (Figure 36(b)). After mechanical stimulation AO is released from granules together with the mucins. As a result of the mucin unfolding the concentration drops and emission is shifts to the green, which shows the volume increase of mucin (Figure 36(a)). The bottom parts of Figure 36(a) and (b) represent fluorescence emission spectra and lifetime measurements for Acridine Orange in the solution that contains mucins of concentration 0.05 g/mL.

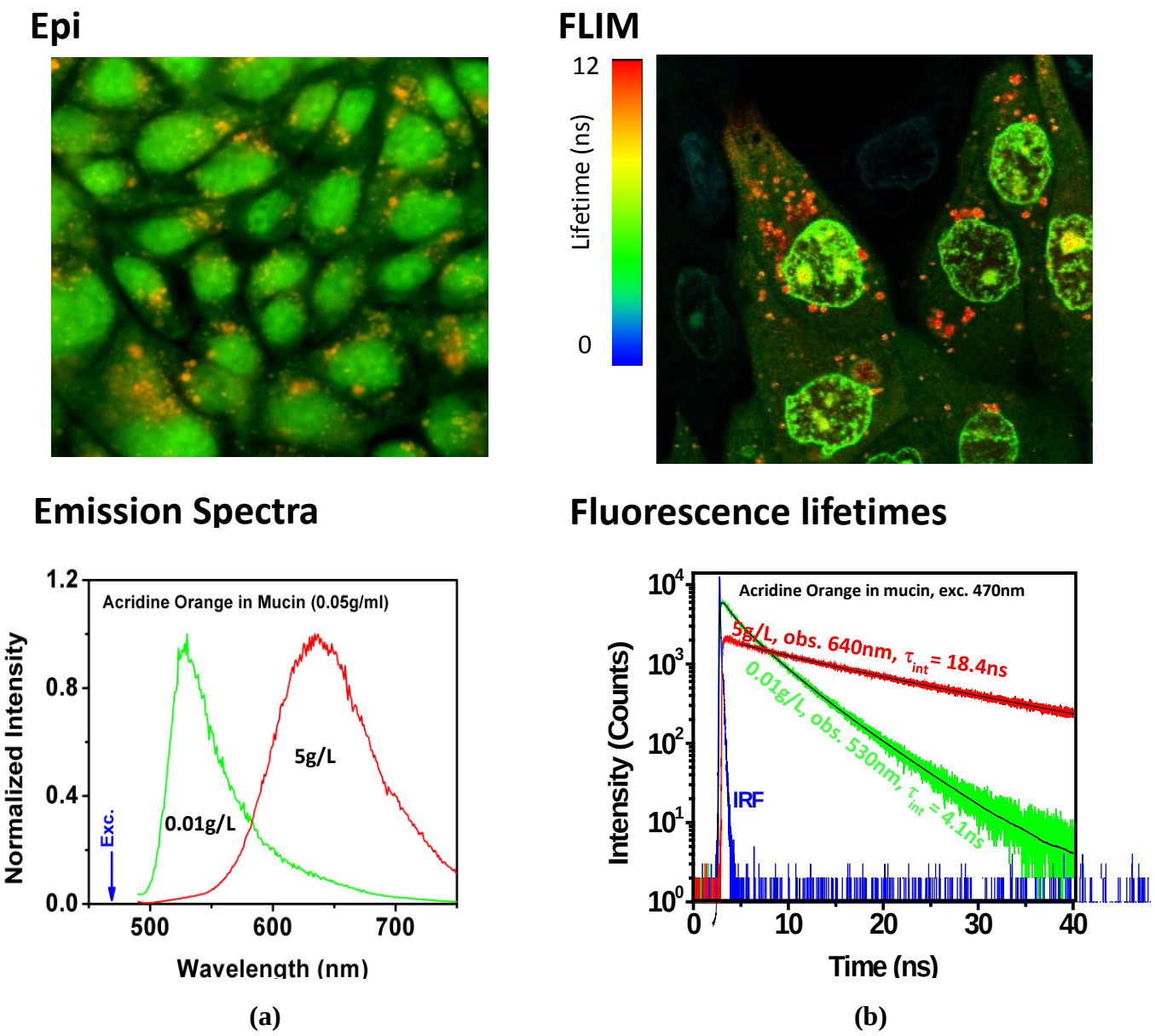

Figure 36. Calu 3 cell stained with Acridine Orange. (a) Epi image and emission spectra, (b) FLIM image and lifetimes

PLANS FOR FUTURE EXPERIMENTS

- Perform absorption spectra, fluorescent spectra and fluorescent lifetimes measurements of different concentrations of the AO for different temperatures (0°C, 37°C, 50°C)

- Perform absorption spectra, fluorescent spectra and fluorescent lifetimes measurements of different concentrations of the AO for different pH levels (5, 7.4, 9)

- Using TIRF microscope and ratiometric technique study exocytotic process of the mucin in the Calu 3 cells and CF-like Calu 3 cells

REFERENCES:

1. O.S.Wolbeis, M.Hof, R.Hutterer, V.Fidler. *Fluorescent Spectroscopy in Biology*, ISBN 3-540-22338-X, 1-2pp.
2. Bernard Valeur and Mario N.Berberan-Santos. *Molecular fluorescence, Second edition*, Print ISBN 978-3-527-32837-6, Wiley 2012, p.40
3. Rodney Loudon. *The Quantum Theory of Light*, ISBN 0-19-850177, Oxford University Press, p.26
4. Joseph R.Lakowich. *Principles of Fluorescence Spectroscopy, Second edition*. ISBN 0-306-46093-9, 1999 Kluwer Academic/ Plenum Publishers, New York, 10-11 pp.
5. O.S.Wolbeis, M.Hof, R.Hutterer, V.Fidler, *Fluorescent Spectroscopy in Biology*, ISBN 3-540-22338-X, 105p.
6. Bernard Valeur and Mario N.Berberan-Santos. *Molecular fluorescence, Second edition*, Print ISBN 978-3-527-32837-6, Wiley 2012, p.265
7. Joseph R.Lakowich. *Principles of Fluorescence Spectroscopy, Second edition*. ISBN 0-306-46093-9, 1999 Kluwer Academic/ Plenum Publishers, New York, 96 p.
8. Wolfgang Becker, *TCSPC Handbook, 4th edition*. Becker & Hickl GmbH 2010, p.39
9. Mikhail Y. Berezin and Samuel Achilefu. *Fluorescence Lifetime Measurements and Biological Imaginag.* Chem.-Rev.,2010,10,2641-26-84
10. Yi Chun-Chen, Robert M Clegg, *Fluorecence lifetime-resolved imaging* Photosynth Res (2009) 102:143-155
11. Philip R. Bevington. *Data Reduction and Error Analysis in Physical Sciences*. McGraw – Hill Book Company 1969
12. Joseph R.Lakowich. *Principles of Fluorescence Spectroscopy, Second edition*. ISBN 0-306-46093-9, 1999 Kluwer Academic/ Plenum Publishers, New York, 119-120 pp.
13. *PicoQuant FT 300 brochure* (PicoQuant website)
14. Michael E.Lamn and David M.Neville. *The Dimer Spectrum of Acridine Orange Hydrochloride*. The Journal of Physical Chemistry, Volume 69,Number 11, November 1965
15. Shohren Nafisi, Ali Akbar Saboury, Nahid Keramat, Jean-Francois Neault, Heidar-Ali Tajmir-Riahi. *Stability and structural features of DNA intercalation with ethidium bromide, acridine orange and methylene blue*. Journal of Molecular Structure, May 2006

16. S.A. Korolenko, S.Ya. Adamyan, T.N. Belyaeva, T.P. Mozhenok. *Acridine orange accumulation in acid organelles of normal and vacuolated frog skeletal muscle fibers*. Cell Biology International 30(2006) 933-939
17. M.M. Murad. *Fluorescence Analysis of Acridine Orange Absorbate at the Water/N-Heptane Interface, Bulk and Interface*. Journal of Fluorescence, Vol.9, #3,1999
18. P.Verdugo. *Supramolecular Dynamics of Mucus*. Cold Spring Harb Med 2012;2:a009597
19. *COPD*, American Lung Association website
20. *CF*, American Lung Association website
21. Brian Button, Li-Heng Cai, Camille Ehre, Mehmet Kesimer, David B. Hill, John K. Sheehan, Richard C.Boucher, Michael Rubinstein. *A Periciliary Brush Promotes the Lung Health by Separating the Mucus Layer from Airway Epithelia*. Science Vol.337, 24 August 2012
22. Rahul Kuver, Johanne Henriette Klinkspoor, William R.A.Osborne and Sum P.Lee. *Mucous granule exocytosis and CFTR expression in gallbladder epithelium*. Glycobiology vol. 10, no2 pp. 149-157,2000
23. Joseph R.Lakowich. *Principles of Fluorescence Spectroscopy, Second edition*. ISBN 0-306-46093-9, 1999 Kluwer Academic/ Plenum Publishers, New York, 129-131 pp.
24. Joseph R.Lakowich. *Principles of Fluorescence Spectroscopy, Second edition*. ISBN 0-306-46093-9, 1999 Kluwer Academic/ Plenum Publishers, New York, 52-53 pp.
25. A.T.R. Williams, S.A Winfield and J.M.Miller. *Relative fluorescence quantum yields using a computer controlled luminescence spectrometer*. Analyst,1983,108,1067
26. Daniel Axelrod, Thomas P.Burghardt, Nancy L. Thompson. *Total Internal Reflection Fluorescence*. Biophys. Bioeng. 1984.13:247-268
27. *Olympus Application Note* (Olympus website)
28. Steyer J. and Almers, W. *Transport, docking and exocytosis of single secretory granules in live chromaffin cells*. Nature: 388, 474 (1997).
29. Rogers, DF, Respir Care. *Physiology of Airway Mucus Secretion and Pathophysiology of Hypersecretion*. 2007 Sep;52(9):1134-46; discussion 1146-9. Review

VITA

PERSONAL

Dmytro Shumilov
Gorlovka, Ukraine
02-February-1989
Single, no children

EDUCATION

August 2010 – present student	TCU, Department of Physics and Astronomy, graduate
Sep. 2009-June 2010	Kharkiv National University Department of Physics and Technology. Chair of Physical Technology Bachelor of Science, Physics
Sep.1996-June 2006	Gorlovka Secondary School No. 40, Gorlovka, Ukraine

PROFESSIONAL EXPERIENCE

01 July – 01 September 2009	Practical experience on the Chair of Physical Technologies, working with vacuum equipment.
01 September 2009 –30 June 2010	Science Center “Kharkov National University”. Work on problems concerning supercooling during crystallization of thin island films.
1 April 2010 – 30 June 2010	Science Center “Kharkov National University”, Laboratory of Microstructure Investigation. Laboratory technician.
20 August 2010 – present	Department of Physics and Astronomy, research assistant, teaching assistant

ABSTRACT

NEW APPLICATION OF ACRIDINE ORANGE TO STUDY BIOPHYSICS OF EXOCYTOTIC PROCESSES IN CELL

By Dmytro Shumilov, M.S., 2013
Department of Physics and Astronomy
Texas Christian University

Thesis Advisor:

Dr. Zygmunt (Karol) Gryczynski, Professor – Physics Biomedical

Mucus secretion is the first-line of defence against the barrage of irritants inhaled into human lungs, but abnormally thick and viscous mucus results in many respiratory diseases. Investigation of processes underlying mucus pathology is hampered, in part, by lack of appropriate experimental tools for labeling and studying mucin granule secretion from live cells with high sensitivity and temporal resolution. Fluorescence spectra and fluorescence lifetime of AO measurements reveal significant changes due to aggregation, and this properties can be useful for determination of mucus expansion.

In this report I present original spectroscopic properties of acridine orange (AO) which could be utilized to study granule release and mucin swelling with novel fluorescence imaging approaches. To explore fluorescent properties we measured the quantum yield and extinction coefficient and lifetimes.